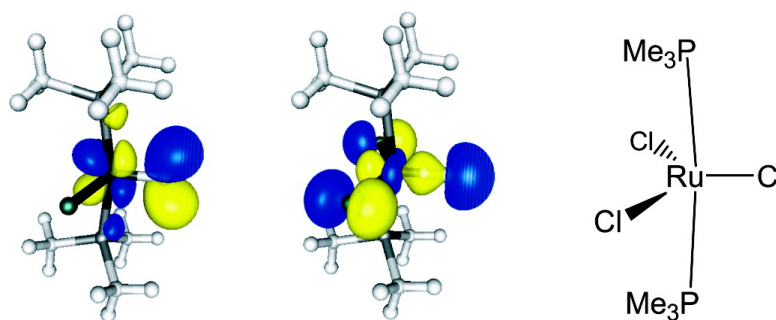


Carbon Complexes as Electronically and Sterically Tunable Analogues of Carbon Monoxide in Coordination Chemistry

Andreas Krapp, and Gernot Frenking

J. Am. Chem. Soc., **2008**, 130 (49), 16646-16658 • DOI: 10.1021/ja8047915 • Publication Date (Web): 17 November 2008

Downloaded from <http://pubs.acs.org> on February 8, 2009



More About This Article

Additional resources and features associated with this article are available within the HTML version:

- Supporting Information
- Access to high resolution figures
- Links to articles and content related to this article
- Copyright permission to reproduce figures and/or text from this article

[View the Full Text HTML](#)



Carbon Complexes as Electronically and Sterically Tunable Analogues of Carbon Monoxide in Coordination Chemistry

Andreas Krapp^{*,†,‡} and Gernot Frenking^{*,†}

Philipps-Universität Marburg, Fachbereich Chemie, Hans-Meerwein-Strasse, D-35032 Marburg, Germany, and Senter for teoretisk og beregningsorientert kjemi, Kjemisk institutt, Universitetet i Oslo, Postboks 1033 Blindern, 0315 Oslo, Norway

Received June 23, 2008; E-mail: frenking@chemie.uni-marburg.de

Abstract: Quantum chemical calculations at DFT (BP86) and ab initio levels (CCSD(T)) have been carried out for transition metal carbon complexes $[MX_2(PR_3)_2(C)]$ with various combinations of $M = Fe, Ru, Os, X = F, Cl, Br, I$, and $R = H, Me, Ph, Cyc$. Calculations have also been performed for $[RuCl_2(PMe_3)(NHC)(C)]$ and $[RuCl_2(NHC)_2(C)]$ where NHC = *N*-heterocyclic carbene and for $[M(Por)(C)]$ ($M = Fe, Ru, Os$; Por = porphyrin). The properties of the carbon complexes as donor ligands were studied by calculating the geometries and bond dissociation energies of the Lewis acid–base adducts with the Lewis acids $M(CO)_5$ ($M = Cr, Mo, W$), $PdCl_2SMe_2$, BH_3 , BCl_3 , and $Fe_2(CO)_8$. The latter species are compared to the analogous CO complexes. The nature of the donor–acceptor interactions between the Lewis acids LA and carbon complexes $[TM]C-LA$ is compared to the bonding in $OC-LA$. The bonding analysis was carried out with charge- and energy-partitioning methods. The bond strength and the donor–acceptor properties of metal carbon complexes closely resemble those of CO, and thus carbon complexes may be considered as electronically tuneable analogues of carbon monoxide. Similar properties are also calculated for the porphyrin carbon complexes **10MC**, which bind more strongly and are slightly stronger π acceptors than the $[(X_2(R)_2)M(C)]$ species. The carbon complexes $[(X_2(R)_2)M(C)]$ are slightly weaker π acceptors than CO, and thus they tend to have slightly weaker bonds than CO in group-6 donor–acceptor complexes. The calculations suggest that bond energies of carbon complexes as ligands with d^{10} transition metals are larger than those of CO. The theoretical results let it seem possible that adducts with more than one carbon complex as ligands may be synthesized and that even homoleptic complexes may be prepared.

Introduction

Carbon monoxide (CO) is a ubiquitous ligand in transition metal (TM) chemistry. Since the first preparation of the carbonyl complex $[PtCl_2(CO)]_2$ by Schützenberger in 1868,¹ innumerable examples of compounds with CO as ligand have been synthesized. The structural diversity of homoleptic TM carbonyl complexes ranges from monocentric compounds $M(CO)_x$ to clusters $M_y(CO)_x$ in which CO coordinates either in a η^1 -end-on mode or in the η^2 - or η^3 -bridging mode. Carbonyl complexes are of wide interest as reagents in synthetic chemistry (e.g., Collman's reagent $Na_2[Fe(CO)_4]$ ² is used for the functionalization of organic halogen compounds), and they are known to be intermediates in homogeneous catalysis.³ Furthermore, carbonyl complexes serve as starting materials for the synthesis of other low-valent TM complexes. Given the importance of CO, it is clear that a ligand that has bonding properties comparable to those of CO but can be tuned in its electronic and steric properties could be very interesting for coordination chemistry.

The most obvious alternatives to CO are valence-isoelectronic molecules like N_2 , NO^+ , CN^- , CS , CSe , CTe , or CNR .

For all of these molecules, TM complexes are known,³ but from the available experimental data it becomes clear that none of these ligands is as versatile as CO. Inspired by this finding, the groups of Bickelhaupt, Baerends, and Hoffmann (BBH) studied intensively the bonding capabilities of the ligands N_2 , BF , BNR_2 , BO^- , and SiO ,^{4–6} which are valence-isoelectronic to CO. BBH suggested that the reason for the special character of CO is the balance between its internal stability and the excellent binding property. Both factors are the consequence of an intermediate energy gap between the highest occupied molecular orbital (HOMO) and the lowest unoccupied molecular orbital (LUMO). The HOMO of CO is a σ -orbital with a large amplitude at the carbon atom suitable for $OC \rightarrow TM$ σ -donation, and the LUMO is a π^* -orbital that allows for $OC \leftarrow TM$ π -backdonation according to the Dewar–Chatt–Duncanson (DCD) model.^{7–9} BBH predicted that BF would be a valuable alternative to CO

(4) Ehlers, A. W.; Baerends, E. J.; Bickelhaupt, F. M.; Radius, U. *Chem.-Eur. J.* **1998**, *4*, 210.

(5) Radius, U.; Bickelhaupt, F. M.; Ehlers, A. W.; Goldberg, N.; Hoffmann, R. *Inorg. Chem.* **1998**, *37*, 1080.

(6) Bickelhaupt, F. M.; Radius, U.; Ehlers, A. W.; Hoffmann, R.; Baerends, E. J. *New J. Chem.* **1998**, *22*, 1.

(7) Dewar, M. J. S. *Bull. Soc. Chim. Fr.* **1951**, *18*, C79.

(8) Chatt, J.; Duncanson, L. A. *J. Chem. Soc.* **1953**, 2929.

(9) (a) Frenking, G. *J. Organomet. Chem.* **2001**, *635*, 9. (b) Frenking, G. In *Modern Coordination Chemistry: The Legacy of Joseph Chatt*; Leigh, G. J., Winterton, N., Eds.; The Royal Society: London, 2002; p 111.

[†] Philipps-Universität Marburg.

[‡] Universitetet i Oslo.

(1) Schützenberger, P. *Ann. Chim. Phys. (Paris)* **1868**, *15*, 100.

(2) Collman, J. P. *Acc. Chem. Res.* **1975**, *8*, 342.

(3) Elschenbroich, C. *Organometallics*, 3rd ed.; Wiley-VCH: Weinheim, 2006.

and that TM–fluoroborylene complexes should even exhibit enhanced stability, because the σ -donor capability and the π -acceptor capability of BF should be higher than that of CO due to the energetically higher lying HOMO and the lower lying LUMO of BF.^{4–6} Up to now, there is no example of a fluoroborylene complex that could become synthesized, which is probably the consequence of the fact that the boron center is highly susceptible to nucleophilic attack. However, a number of sterically crowded and electronically stabilized borylene complexes have been synthesized by Braunschweig and co-workers,¹⁰ but only four haloborylene complexes could become isolated: $[(\mu\text{-BCl})\{\eta^5\text{-C}_5\text{H}_4\text{Me}\}\text{Mn}(\text{CO})_2\}_2]$,¹¹ $[(\mu\text{-BCl})\{\eta^5\text{-C}_5\text{H}_5\}\text{Fe}(\text{CO})_2\}_2]$,¹¹ and $[(\mu\text{-BX})\{\text{Mn}(\text{CO})_5\}_2]$ (X = Cl, Br).¹¹

The advances in borylene chemistry beautifully exemplify that inspiration by the orbital structure can be very fruitful. Yet the alternatives to CO are not restricted to the above presented examples of small isoelectronic main-group molecules. As BBH have shown, the “archimedic point” in the coordination chemistry of carbon monoxide is its orbital structure. Thus, looking for TM complexes that have an orbital structure similar to CO could be a possible alternative to find analogues of CO that allow for a real fine-tuning of both the electronic and the steric properties, because TM complexes bear further adjustable ligands L. Thus, the goal is to find a complex [TM]–C that is isolobal¹² to CO.

During our recent computational study on the bonding situation in TM complexes with a naked carbon atom as terminal ligand¹³ (which are named carbon complexes by us),¹⁵ we noticed that the frontier orbitals of the model complex $[(\text{Cl}_2(\text{PMe}_3)_2\text{Ru}(\text{C}))]$ resemble the HOMO and LUMO of CO in number, symmetry, energy, shape, and occupancy. This finding suggests that CO and $[(\text{Cl}_2(\text{PMe}_3)_2\text{Ru}(\text{C}))]$ are isolobal, which also means that the oxygen atom and the $[(\text{Cl}_2(\text{PMe}_3)_2\text{Ru})]$ unit are isolobal.¹⁶ The latter observation was also made by Johnson and co-workers in their recent, detailed study on terminal carbon complexes.¹⁴ It thus seems possible that $[(\text{Cl}_2(\text{PMe}_3)_2\text{Ru}(\text{C}))]$ and CO show similar coordination chemistry.

Experimentally, three transition metal carbon complexes have been synthesized, and their structures were determined by X-ray

diffraction: $[(\text{Cl}_2(\text{PCyc}_3)_2\text{Ru}(\text{C}))]$ (Cyc = cyclohexyl),^{17–19} $[(\text{Cl}_2(\text{PCyc}_3)(\text{L})\text{Ru}(\text{C}))]$ (L = 1, 3-dimesityl-4,5-dihydroimidazol-2-ylidene),¹⁷ and $[(\text{Cl}_2(\text{PCyc}_3)_2\text{Os}(\text{C}))]$.²⁰ Further carbon complexes have been reported, but there is no X-ray structure available.²⁷ There are also examples of coordination compounds known where a carbon complex acts as Lewis base through the carbon ligand.^{18,21} Grubbs and co-workers¹⁸ isolated and structurally characterized $[(\text{Cl}_2(\text{PCyc}_3)_2\text{Ru}(\text{C}))\text{-PdCl}_2\text{SMe}_2]$. In the same article,¹⁸ the authors reported about the NMR chemical data of the compound $[(\text{Cl}_2(\text{PCyc}_3)_2\text{Ru}(\text{C}))\text{-Mo}(\text{CO})_5]$, which could, however, not become isolated so far. In 1990, Beck and co-workers reported about the crystal structure of $[(\text{Por}')\text{-Fe}(\text{C})\text{Re}(\text{CO})_4\text{Re}(\text{CO})_5]$ (Por' = 5,10,15,20-tetraphenylporphyrin), which can be described as a donor–acceptor complex between the carbon complex $[(\text{Por}')\text{Fe}(\text{C})]$ and the Lewis acid $[\text{Re}(\text{CO})_4\text{Re}(\text{CO})_5]$. We want to point out that both $[(\text{Cl}_2(\text{PCyc}_3)_2\text{Ru}(\text{C}))]$ and $[(\text{Por}')\text{Fe}(\text{C})]$ bear $d^6\text{ML}_4$ -fragments, which supports the proposal that CO and $[\text{L}_4\text{M}\text{-C}]$ complexes with d^6 -metals M are isolobal. The experimental data confirm that $[\text{L}_4\text{M}(\text{C})]$ compounds can act as ligands that bind to a Lewis acid.

Besides these three structural studies, nothing is known about the bonding of carbon complexes to Lewis acids, and no attempt has been made to connect the chemistry of CO with the one of carbon complexes. It is the goal of this Article to establish the analogy between CO and carbon complexes and to show that the variability of the electronic and steric properties of the carbon complexes allows one to fine-tune their coordination behavior.

We set out a computational study to shed light on the bonding capabilities of CO and the carbon complexes (d^6) $\text{ML}_4(\text{C})$ with various Lewis acids. The following carbon complexes were considered: $[\text{RuCl}_2(\text{PR}_3)_2(\text{C})]$ (R = H, Me, Ph, Cyc; Me = methyl; Ph = phenyl; Cyc = cyclohexyl), $[\text{MCl}_2(\text{PMe}_3)_2(\text{C})]$ (M = Fe, Ru, Os), $[\text{RuX}_2(\text{PMe}_3)_2(\text{C})]$ (X = F, Cl, Br, I), $[\text{RuCl}_2(\text{PMe}_3)(\text{NHC})(\text{C})]$ (NHC = 1,3-dimethylimidazolidin-2-ylidene), $[\text{RuCl}_2(\text{NHC})_2(\text{C})]$, and $[\text{M}(\text{Por})(\text{C})]$ (M = Fe, Ru, Os; Por = porphyrin). Table 1 gives an overview of the carbon complexes **1RuC**–**10RuC**, **1FeC**, **1OsC**, **10FeC**, and **10OsC**, which have been studied in this work. This set of carbon complexes allows for the study of the influence of the ligand sphere and the central metal on the bonding capabilities. As Lewis acids, we chose $\text{M}(\text{CO})_5$ (M = Cr, Mo, W), BCl_3 , BH_3 , and $\text{PdCl}_2\text{SMe}_2$, which permits the variation of the type of Lewis acid (main group, transition metal).

- (10) (a) Braunschweig, H.; Kollann, C.; Rais, D. *Angew. Chem.* **2006**, *118*, 5380. (b) Braunschweig, H.; Kollann, C.; Rais, D. *Angew. Chem., Int. Ed.* **2006**, *45*, 5254.
- (11) (a) Braunschweig, H.; Colling, M.; Hu, C.; Radacki, K. *Angew. Chem.* **2002**, *114*, 1415. (b) Braunschweig, H.; Colling, M.; Hu, C.; Radacki, K. *Angew. Chem., Int. Ed.* **2002**, *41*, 1359. (c) Bissinger, P.; Braunschweig, H.; Seeler, F. *Organometallics* **2007**, *26*, 4700.
- (12) (a) Hoffmann, R. *Angew. Chem.* **1982**, *94*, 725. (b) Hoffmann, R. *Angew. Chem., Int. Ed. Engl.* **1982**, *21*, 711.
- (13) Krapp, A.; Pandey, K. K.; Frenking, G. *J. Am. Chem. Soc.* **2007**, *129*, 7596.
- (14) A theoretical study of thermodynamic considerations in TM complexes with terminal carbon atoms has recently been published by: Gary, J. B.; Buda, C.; Johnson, M. J. A.; Dunietz, B. D. *Organometallics* **2008**, *27*, 814.
- (15) We distinguish between a transition metal carbide and a carbon complex in a manner analogous to that which we use to distinguish between a Schrock-type carbyne (alkylidyne) and a Fischer-type carbyne complex. The former compounds have an electron-sharing triple bond, while the latter complexes have donor–acceptor bonds between the transition metal and the carbyne ligand, which can be discussed with the Dewar–Chatt–Duncanson bonding model. Note that in ref 14 the authors use the term “carbide” to denote all complexes that have a C_1 ligand without reference to the charge it carries. All transition metal carbides that have been isolated so far have a negative charge, and they may also be considered as Schrock-type carbyne anions: (a) Peters, J. C.; Odom, L. A.; Cummins, C. C. *Chem. Commun.* **1997**, 1995. (b) Greco, J. B.; Peters, J. C.; Baker, T. A.; Davis, W. M.; Cummins, C. C.; Wu, G. *J. Am. Chem. Soc.* **2001**, *123*, 5003.

- (16) There is an accepted isolobal relation between the oxygen atom and $d^8 \text{ML}_4$ fragments like $\text{Fe}(\text{CO})_4$.¹² This leads to an isolobal relation between CO and $(\text{CO})_4\text{Fe}(\text{C})$. Up to now, all experimental attempts to isolate $\text{Fe}(\text{CO})_4(\text{C})$ failed. See: (a) Petz, W.; Weller, F. *Organometallics* **1993**, *12*, 4056. (b) Chen, Y.; Petz, W.; Frenking, G. *Organometallics* **2000**, *19*, 2698. $\text{Fe}(\text{CO})_4(\text{C})$ is probably a highly reactive species. This is in contrast to the high stability and moderate reactivity of the $[(\text{Cl}_2(\text{PR}_3)_2\text{Ru}(\text{C}))]$ molecule, which reminds one of the high stability and the inertness of the CO molecule itself. Given the orbital structure and the chemical behavior, we think that the isolobal relation between the oxygen atom and a $d^6 \text{ML}_4$ fragment could be more appropriate.
- (17) Carlson, R. G.; Gile, M. A.; Heppert, J. A.; Mason, M. H.; Powell, D. R.; Velde, D. V.; Vilain, J. M. *J. Am. Chem. Soc.* **2002**, *124*, 1580.
- (18) Hejl, A.; Trnka, T. M.; Day, M. W.; Grubbs, R. H. *Chem. Commun.* **2002**, 2524.
- (19) Caskey, S. R.; Stewart, M. H.; Kivela, J. E.; Sootsman, J. R.; Johnson, M. J. A.; Kampf, J. W. *J. Am. Chem. Soc.* **2005**, *127*, 16750.
- (20) Stewart, M. H.; Johnson, M. J. A.; Kampf, J. W. *Organometallics* **2007**, *26*, 5102.
- (21) (a) Beck, W.; Knauer, W.; Robl, C. *Angew. Chem.* **1990**, *102*, 331. (b) Beck, W.; Knauer, W.; Robl, C. *Angew. Chem., Int. Ed. Engl.* **1990**, *29*, 318.

Table 1. Overview of the Investigated Carbon Complexes

molecule	no.
RuCl ₂ (PMe ₃) ₂ (C)	1RuC
FeCl ₂ (PMe ₃) ₂ (C)	1FeC
OsCl ₂ (PMe ₃) ₂ (C)	1OsC
RuCl ₂ (PH ₃) ₂ (C)	2RuC
RuCl ₂ (PPH ₃) ₂ (C)	3RuC
RuCl ₂ (PCyc ₃) ₂ (C)	4RuC
RuF ₂ (PMe ₃) ₂ (C)	5RuC
RuBr ₂ (PMe ₃) ₂ (C)	6RuC
RuI ₂ (PMe ₃) ₂ (C)	7RuC
RuCl ₂ (PMe ₃)(NHC)(C)	8RuC
RuCl ₂ (NHC) ₂ (C)	9RuC
Ru(Por)(C)	10RuC
Fe(Por)(C)	10FeC
Os(Por)(C)	10OsC

Experimental studies have shown that CO may bind in transition metal complexes end-on (η^1) through the carbon atom, but η^2 - and η^3 -binding modes bridging several metal atoms are also known.³ To test whether the isolobal carbon complexes can also serve as bridging ligands, we included in our study the complex [Fe₂(CO)₉] and the analogous molecule [RuCl₂(PMe₃)₂(C)–Fe₂(CO)₈] where the carbon compound [RuCl₂(PMe₃)₂(C)] binds in the η^2 -coordination mode. Another interesting question is whether more than one carbon complex could bind to a TM as is the case of carbon monoxide, which forms numerous homoleptic compounds M(CO)_n. We therefore studied also the series of coordination compounds W(CO)_(6-n)–[(RuCl₂(PH₃)₂(C))_n] ($n = 0–6$).

We report on the equilibrium structures and bond dissociation energies of the carbon complexes **1RuC**–LA to **10OsC**–LA, where the Lewis acid LA is Cr(CO)₅, Mo(CO)₅, W(CO)₅, PdCl₂SMe₂, BH₃, BCl₃. The carbon complexes are compared to the isolobal species OC–LA and also with SC–W(CO)₅ and FB–W(CO)₅. An important part of the work consists of the analysis of the bonding situation, which has been investigated with energy- and charge-partitioning methods.

Computational Details

The geometries of the molecules have been fully optimized using density functional theory (DFT) at the BP86^{33,34} level using the RI (resolution of identity) approximation³⁵ in conjunction with the Weigend/Ahlrichs basis sets def2-TZVPP^{36,37} for all atoms. The notation def2-TZVPP indicates all-electron basis sets for the atoms except for Ru, Os, Mo, W, and Pd where a quasi-relativistic effective core potential (ECP)³⁸ is combined with a TZVPP valence basis set.³⁶ This level of theory is denoted as BP86/TZVPP. The vibrational frequencies were calculated at this level of theory. The geometry, energy, and frequency calculations have been carried out with the program package Turbomole.³⁹ For some molecules with very bulky phosphine substituents, we could not perform vibrational frequency calculations because of computer limitations. The geometry optimizations of the latter species were carried out with C₁ symmetry. Therefore, we think that the molecules are also minima on the potential energy surfaces. We also calculated the energies of some of the BP86/TZVPP optimized structures using coupled cluster theory²² at the CCSD(T) level^{23–26} in conjunction with the above TZVPP basis sets. The CCSD(T) calculations were carried out with the program MolPro2006.⁴⁰

The electronic structure of the molecules was analyzed with different methods. For the charge analysis, we used the natural bond orbital (NBO) of Weinhold³² as implemented in the Turbomole program. The energy decomposition analysis (EDA)^{28,41–45} calculations on the BP86/TZVPP optimized structures have been performed at the BP86 level using uncontracted Slater-type orbitals (STOs), which have TZ2P quality.⁴⁶ Scalar relativistic effects have been considered using the zero-order regular approximation (ZORA).^{72–76} The latter calculations were carried out with the program package ADF.^{47,48}

The focus of the EDA^{28–31} is the instantaneous interaction energy ΔE_{int} , which is the energy difference between the molecule and the fragments with the frozen geometry of the complex. The interaction energy is divided into three main components:

$$\Delta E_{\text{int}} = \Delta E_{\text{elstat}} + \Delta E_{\text{Pauli}} + \Delta E_{\text{orb}}$$

The term ΔE_{elstat} gives the electrostatic interaction energy between the fragments that are calculated with a frozen density distribution in the geometry of the complex. The Pauli repulsion (ΔE_{Pauli}) arises as the energy change associated with the transformation from the superposition of the unperturbed electron densities of fragments $\rho_A + \rho_B$ to the wave function $\Psi^0 = N\hat{A}\{\Psi_A \cdot \Psi_B\}$, which properly obeys the Pauli principle through explicit antisymmetrization (\hat{A}) and renormalization (N) of the product wave function. It comprises the destabilizing interactions between electrons on either fragment

- (27) See refs 19 and 20 and the following: (a) Romero, P. E.; Piers, W. E.; McDonald, R. *Angew. Chem.* **2004**, *116*, 6287. (b) Romero, P. E.; Piers, W. E.; McDonald, R. *Angew. Chem., Int. Ed.* **2004**, *43*, 6161. (c) van der Eide, E. F.; Romero, P. E.; Piers, W. E. *J. Am. Chem. Soc.* **2008**, *130*, 4485.
- (28) Bickelhaupt, F. M.; Baerends, E. J. In *Reviews in Computational Chemistry*; Lipkowitz, K. B., Boyd, D. B., Eds.; Wiley-VCH: New York, 2000; Vol. 15, p 1.
- (29) Frenking, G.; Wichmann, K.; Fröhlich, N.; Loschen, C.; Lein, M.; Frunzke, J.; Rayon, V. M. *Coord. Chem. Rev.* **2003**, *238–239*, 55.
- (30) Lein, M.; Szabo, A.; Kovacs, A.; Frenking, G. *Faraday Discuss.* **2003**, *124*, 365.
- (31) Lein, M.; Frenking, G. In *Theory and Applications of Computational Chemistry. The First 40 Years*; Dykstra, C. E., Frenking, G., Kim, K. S., Scuseria, G., Eds.; Elsevier: Amsterdam, 2005; p 367.
- (32) Reed, A. E.; Curtiss, L. A.; Weinhold, F. *Chem. Rev.* **1988**, *88*, 899.
- (33) Becke, A. D. *Phys. Rev. A* **1988**, *38*, 3098.
- (34) Perdew, J. P. *Phys. Rev. B* **1986**, *33*, 8822.
- (35) Eichkorn, K.; Treutler, O.; Öhm, H.; Häser, M.; Ahlrichs, R. *Chem. Phys. Lett.* **1995**, *242*, 652.
- (36) Weigend, F.; Ahlrichs, R. *Phys. Chem. Chem. Phys.* **2005**, *7*, 3297.
- (37) Weigend, F. *Phys. Chem. Chem. Phys.* **2006**, *8*, 1057.
- (38) Andrae, D.; Haeussermann, U.; Dolg, M.; Stoll, H.; Preuss, H. *Theor. Chim. Acta* **1990**, *77*, 123.
- (39) Ahlrichs, R.; Bär, M.; Häser, M.; Horn, H.; Kölmel, C. *Chem. Phys. Lett.* **1989**, *162*, 165.
- (40) Werner, H.-J.; Knowles, P. J.; Lindh, R.; Manby, F. R.; Schütz, M.; Celani, P.; Korona, T.; Rauhut, G.; Amos, R. D.; Bernhardsson, A.; Berning, A.; Cooper, D. L.; Deegan, M. J. O.; Dobbyn, A. J.; Eckert, F.; Hampel, C.; Hetzer, G.; Lloyd, A. W.; McNicholas, S. J.; Meyer, W.; Mura, M. E.; Nicklass, A.; Palmieri, P.; Pitzer, R.; Schumann, U.; Stoll, H.; Stone, A. J.; Tarroni, R.; Thorsteinsson, T. MOLPRO, version 2006.1, a package of ab initio programs; see <http://www.molpro.net>.
- (41) Ziegler, T.; Rauk, A. *Inorg. Chem.* **1979**, *18*, 1755.
- (42) Ziegler, T.; Rauk, A. *Inorg. Chem.* **1979**, *18*, 1558.
- (43) Ziegler, T.; Rauk, A. *Theor. Chim. Acta* **1977**, *46*, 1.
- (44) Kitaura, K.; Morokuma, K. *Int. J. Quantum Chem.* **1976**, *10*, 325.
- (45) Morokuma, K. *J. Chem. Phys.* **1971**, *55*, 1236.
- (46) Snijders, J. G.; Baerends, E. J.; Vernooijs, P. *At. Nucl. Data Tables* **1982**, *26*, 483.
- (47) te Velde, G.; Bickelhaupt, F. M.; Baerends, E. J.; Van Gisbergen, S. J. A.; Fonseca Guerra, C.; Snijders, J. G.; Ziegler, T. *J. Comput. Chem.* **2001**, *22*, 931.
- (48) Theoretical Chemistry, Vrije Universiteit, SCM, Amsterdam, The Netherlands; <http://www.scm.com>.
- (49) We also studied the staggered C_{2v} symmetric conformation, which is almost isoenergetic but shows one very small imaginary mode that corresponds to the rotation towards the eclipsed conformation.

(22) Cizek, J. *J. Chem. Phys.* **1966**, *45*, 4256.

(23) Bartlett, R. J.; Purvis, G. D. *Int. J. Quantum Chem.* **1978**, *14*, 516.

(24) (a) Pople, J. A.; Krishnan, R.; Schlegel, H. B.; Binkley, J. S. *Int. J. Quantum Chem.* **1978**, *14*, 545. (b) Pople, J. A.; Head-Gordon, M.; Raghavachari, K. *J. Chem. Phys.* **1987**, *87*, 5968.

(25) Purvis, G. D.; Bartlett, R. J. *J. Chem. Phys.* **1982**, *76*, 1910.

(26) Hampel, C.; Peterson, K.; Werner, H.-J. *Chem. Phys. Lett.* **1992**, *190*, 1.

with the same spin. The stabilizing orbital interaction term ΔE_{orb} is calculated in the final step of the analysis when the orbitals relax to their final form. The latter can be decomposed into contributions from each irreducible representation of the point group of the interacting system. This is very helpful because it directly gives the stabilization, which comes from orbitals having different symmetry. To obtain the bond dissociation energy (D_e), one has to consider the preparation energy ΔE_{prep} , which is the energy difference of the fragments between their equilibrium geometry and the geometry that they have in the molecule:

$$\Delta E (= -D_e) = \Delta E_{\text{int}} + \Delta E_{\text{prep}}$$

Results and Discussion

Geometries and Electronic Structure of the Parent Carbon Complexes. Figure 1 shows the optimized geometries at BP86/TZVPP of the carbon complexes **1RuC–10RuC**, **1FeC**, **1OsC**,

- (50) Jonas, V.; Frenking, G.; Reetz, M. T. *J. Am. Chem. Soc.* **1994**, *116*, 8741.
- (51) The model complex **1RuC–PdCl₂SMe₂** in which the PCyc₃ groups are substituted by PMe₃ differs only in one interesting property from **4RuC–PdCl₂SMe₂**. The Cl–Pd–Cl plane in **4RuC–PdCl₂SMe₂** is quasi parallel to the Cl–Ru–Cl plane, whereas in **1RuC–PdCl₂SMe₂** the two planes are almost perpendicular to each other. We explain the rotation of the PdCl₂SMe₂ group by the different steric demand of the respective phosphine ligands.
- (52) Lewis, K. E.; Golden, D. M.; Smith, G. P. *J. Am. Chem. Soc.* **1984**, *106*, 3905.
- (53) Frenking, G.; Ehlers, A. *J. Am. Chem. Soc.* **1994**, *116*, 1514.
- (54) Li, J.; Schreckenbach, G.; Ziegler, T. *J. Am. Chem. Soc.* **1995**, *117*, 486.
- (55) Li, J.; Schreckenbach, G.; Ziegler, T. *J. Phys. Chem.* **1994**, *98*, 4838.
- (56) Bauschlicher, C. W., Jr.; Ricca, A. *Chem. Phys. Lett.* **1995**, *237*, 14.
- (57) Rablen, P. R. *J. Am. Chem. Soc.* **1997**, *119*, 8350.
- (58) Gilbert, T. M. *J. Phys. Chem. A* **2004**, *108*, 2550.
- (59) Ziegler, T.; Tschinke, V.; Ursenbach, C. *J. Am. Chem. Soc.* **1987**, *109*, 4825.
- (60) Diefenbach, A.; Bickelhaupt, F. M.; Frenking, G. *J. Am. Chem. Soc.* **2000**, *122*, 6449.
- (61) Davidson, E. R.; Kunze, K. L.; Machado, F. B.; Chakravorty, S. *J. Acc. Chem. Res.* **1993**, *26*, 628.
- (62) Mansuy, D. *Pure Appl. Chem.* **1980**, *52*, 681.
- (63) Mansuy, D.; Lecomte, J.-P.; Chottard, J.-C. *Inorg. Chem.* **1981**, *20*, 3119.
- (64) English, D. R.; Hendrickson, D. N.; Suslick, K. S. *Inorg. Chem.* **1983**, *22*, 367.
- (65) Jost, A.; Rees, B. *Acta Crystallogr.* **1975**, *B31*, 2649.
- (66) Venkatachar, A. C.; Taylor, R. C.; Kuczowski, R. L. *J. Mol. Struct.* **1977**, *38*, 17.
- (67) Lias, S. G.; Bartmess, J. E.; Liebman, J. F.; Holmes, J. L.; Levin, R. D.; Mallard, W. G. *J. Phys. Chem. Ref. Data* **1988**, Suppl. 1.
- (68) For a discussion of the bonding situation in CO, see: (a) Frenking, G.; Loschen, C.; Krapp, A.; Fau, S.; Strauss, S. H. *J. Comput. Chem.* **2007**, *28*, 117. (b) Lupinetti, A.; Fau, S.; Frenking, G.; Strauss, S. H. *J. Phys. Chem.* **1997**, *101*, 9551.
- (69) For an alternative interpretation, which suggests that the HOMO of CO is antibonding, see refs 4–6 and: Bickelhaupt, F. M.; Nagle, J. K.; Klemm, W. L. *J. Phys. Chem. A* **2008**, *112*, 2437.
- (70) There are also nonclassical carbonyl complexes where the π -backdonation into the π^* orbital of CO is negligible and the metal–CO orbital interactions come mainly from M–CO σ -donation: (a) Lupinetti, A. J. M.; Frenking, G.; Strauss, S. H. *Angew. Chem.* **1998**, *110*, 2229. (b) Lupinetti, A. J. M.; Frenking, G.; Strauss, S. H. *Angew. Chem., Int. Ed.* **1998**, *37*, 2113.
- (71) An example where the electrostatic interactions rather than the orbital interactions determine the trend in the strength of metal–ligand bonding has been reported in: Frenking, G.; Wichmann, K.; Fröhlich, N.; Grobe, J.; Golla, W.; Le Van, D.; Krebs, B.; Läge, M. *Organometallics* **2002**, *21*, 2921.
- (72) Chang, C.; Pelissier, M.; Durand, P. *Phys. Scr.* **1986**, *34*, 394.
- (73) Heully, J.-L.; Lindgren, I.; Lindroth, E.; Lundquist, S.; Martensson-Pendrill, A.-M. *J. Phys. B* **1986**, *19*, 2799.
- (74) van Lenthe, E.; Baerends, E. J.; Snijders, J. G. *J. Chem. Phys.* **1993**, *99*, 4597.
- (75) van Lenthe, E.; van Leeuwen, R.; Baerends, E. J.; Snijders, J. G. *Int. J. Quantum Chem.* **1996**, *57*, 281.

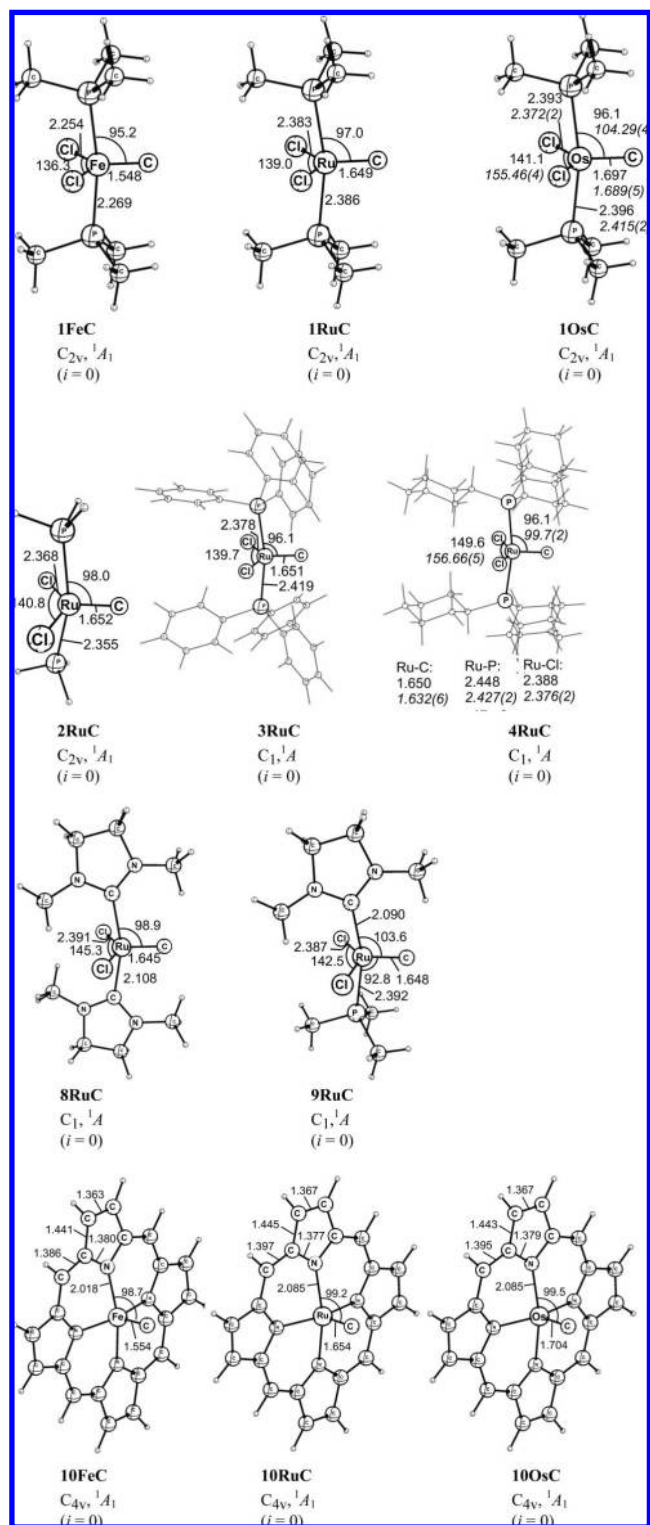


Figure 1. Optimized geometries (BP86/TZVPP) of the carbon complexes **1FeC**, **1RuC**, **1OsC**, **2RuC–4RuC**, **8RuC–10RuC**, **10FeC**, and **10OsC**. The geometries of **5RuC–7RuC** are given in the Supporting Information. Distances in Å, angles in deg. Experimental values are given in italics. In **3RuC** and **4RuC**, the phosphine substituents are drawn with fine gray lines for reasons of clarity. Experimental data (X-ray) for **4RuC** from ref 18; experimental data (X-ray) for [OsCl₂(PCyc)₂(C)] from ref 20.

10FeC, and **10OsC**. Experimental values of complexes **10OsC**²⁰ and **4RuC**,¹⁸ which were taken from the literature, are also given.

The carbon complexes **1RuC–9RuC**, **1FeC**, and **1OsC** all exhibit structures that can be considered as pseudotrigonal bipyramidal geometries with the carbon atom in the equatorial positions. Alternatively, the geometries may also be discussed as distorted square pyramidal forms where the carbon atom occupies the apical position. The porphyrin complexes **10FeC**, **10RuC**, and **10OsC** show tetragonal pyramidal geometries (C_{4v}) with the carbon atom in the apical positions. The optimized structural parameters for **1OsC** and **4RuC** are in good agreement with the experimentally determined data.^{18,20} The variation of the substituents R of the phosphine ligands PR_3 and of the halogen ligands X in $[RuX_2(PR_3)_2(C)]$ (**1RuC**, **3RuC–7RuC**) influence the bond lengths and angles very little (see Figure 1). Substituting one or both phosphine groups in **1RuC** by *N*-heterocyclic carbenes does not disturb the Ru–C bond significantly either (compare **8RuC** and **9RuC** in Figure 1). The porphyrin coordinated compounds **10MC** show M–C bond lengths that are slightly longer than in **1MC**.

The central hypothesis of this work concerns the isobal relationship and thus the similarity between the frontier orbitals of the carbon complexes and CO. Figure 2 displays the highest lying occupied and lowest lying vacant orbitals of **1RuC** and CO. The orbitals of CO show the familiar pattern with HOMO and HOMO–2 being weakly bonding σ orbitals where the HOMO has a large coefficient at the carbon atom. The latter MO has the character of a lone-pair orbital, which is perfectly suited for σ donation. The HOMO–1 and the LUMO are the degenerate π and π^* orbitals of CO. The latter orbital serves as an efficient π -acceptor in classical⁷⁰ carbonyl complexes.

Visual inspection of the frontier orbitals of **1RuC** (Figure 2b) easily identifies σ - and π -orbitals with respect to the Ru–C bond, which closely resemble the orbitals of CO. There are two occupied weakly bonding Ru–C σ -bonding orbitals ($25a_1$ and $26a_1$), which have bonding ($25a_1$) or antibonding ($26a_1$) contributions from the chlorine lone-pair orbitals. Both orbitals have a large coefficient at the terminal carbon atom, which makes $25a_1$ and $26a_1$ efficient σ -donor orbitals. There are three occupied Ru–C π -bonding orbitals ($14b_1$, $16b_1$, and $16b_2$), which can serve as π -donor orbitals like the HOMO–1 of CO. It has been shown that the π -donation of CO in TM carbonyl complexes is negligible.^{59–64} The LUMO+1 and the LUMO+2 of **1RuC** have Ru–C π -antibonding character with a large amplitude on the carbon atom. They are well suited for π -accepting interactions with π -donor ligands. The HOMO, HOMO–1, and LUMO of **1RuC** (not shown in Figure 2b) have very small or zero coefficients at the terminal carbon atoms, and thus they are not relevant for the donor–acceptor interactions with a ligand.

The variation of the metal and the ligands changes the frontier orbital energies of the carbon complexes. Figure 3 shows the energy levels of the relevant σ donor and π^* acceptor orbitals for **1RuC–10RuC**, **1FeC**, **1OsC**, **10FeC**, and **10OsC**. The order of the entries is chosen so that the ligand and metal effects can easily be compared. The energy levels of the occupied donor orbitals refer to the highest lying σ MOs. The π^* acceptor orbitals of **10MC** are degenerate, while they are slightly split for the other carbon complexes. The energy levels of the frontier orbitals of CO and valence isoelectronic CS and BF are shown for comparison.

It becomes obvious that the σ donor orbitals of the carbon complexes, which are in the range between -6 and -7 eV, are

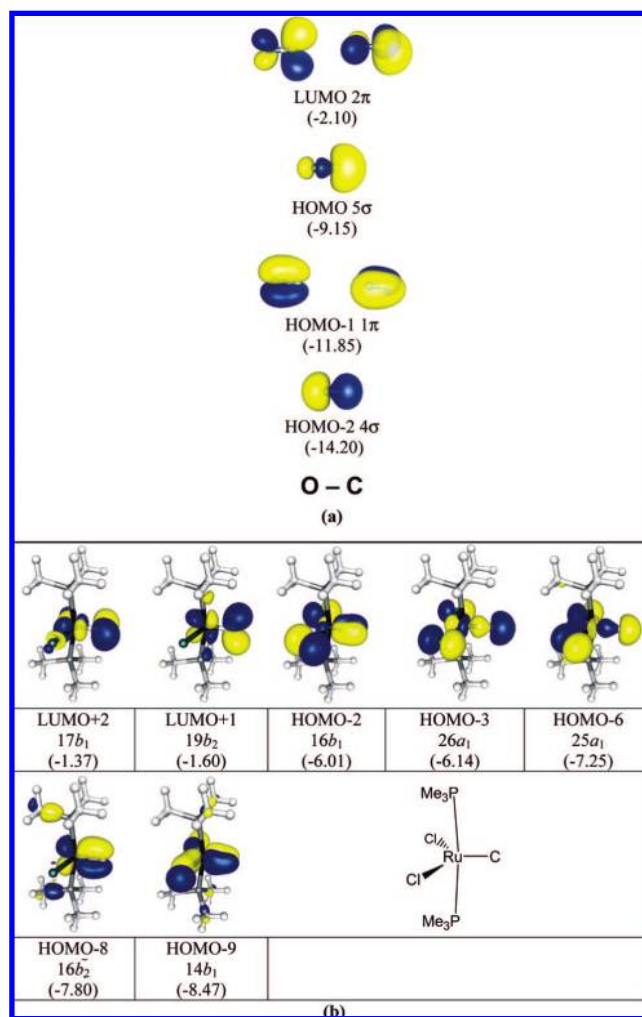


Figure 2. (a) The three highest lying occupied and the lowest lying unoccupied Kohn–Sham molecular orbitals of CO at BP86/TZVPP. Orbital energies in eV. (b) Selected occupied and unoccupied Kohn–Sham molecular orbitals of $[RuCl_2(PMe_3)_2C]$ (**1RuC**) at BP86/TZVPP. Orbital energies in eV.

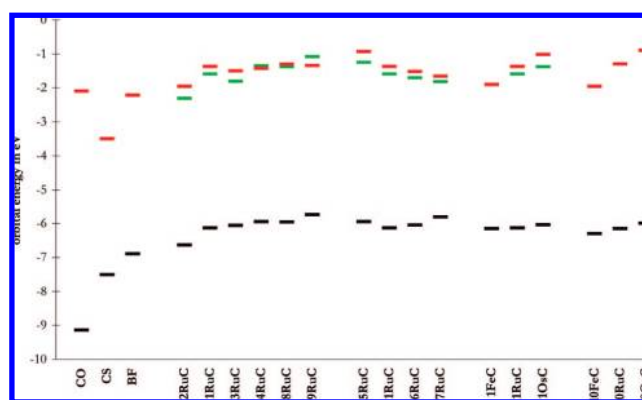


Figure 3. Orbital energies in eV at BP86/TZVPP for CO, CS, BF, and **1RuC–10RuC**, **1FeC**, **1OsC**, **10FeC**, and **10OsC**. The black entries give the occupied σ -orbitals that are analogues to the 5σ HOMO of CO, while the green and red entries give the two unoccupied π -orbitals that are analogues to the degenerate 2π LUMO of CO. For **1MC** ($M = Fe, Ru, Os$) and **5RuC–9RuC**, the π -orbital that lies in the same plane as the Cl, F, Br, I atoms is drawn in green, and the other one is in red.

energetically much higher lying than the σ HOMO of CO, which lies at -9.1 eV. This means that the carbon complexes should

(76) van Lenthe, J. G.; Baerends, E. J.; Snijders, J. G. *J. Chem. Phys.* **1996**, *105*, 6505.

be better donors than CO. The energy levels of the π^* -orbitals of the carbon compounds are comparable to the energy of the π^* LUMO of CO. This means that the carbon complexes should be better electron donors than CO, while the π -acceptor strengths of [TM]–C and CO should be comparable. This rough estimate, which considers only the energy levels of the frontier orbitals, shall be compared to the calculated stabilization that comes from σ and π -orbital interactions in transition metal complexes with [TM]–C and CO as ligands in the next section.

Figure 3 shows that the energy levels of the σ -orbitals of the complexes change less than do the π^* -orbital energies when the metal or the ligand becomes altered. The trend of the π^* -orbital energies suggests that the acceptor strength of the halogen systems **1RuC**, **5RuC**–**7RuC** increases with $F < Cl < Br < I$. The variation of the central metal atom in **1MC** and **10MC** indicates that the π acceptor strength decreases with $Fe > Ru > Os$. The variation of the substituents at PR_3 has only a minor influence on the orbital energies. From the orbital energies, it appears that the donor–acceptor strength of the carbon complexes resembles BF more than CO.

Geometry and Bond Dissociation Energies of Donor–Acceptor Adducts with Carbon Complexes and CO as Ligands. Figure 4 shows the optimized geometries at BP86/TZVPP of the donor–acceptor complexes with [TM]–C as ligand. The geometries of the CO complexes are given in Figure 5. Experimental values of related complexes are also shown in Figures 4 and 5. The optimized geometries of the free Lewis acids $M(CO)_5$ ($M = Cr, Mo, W$), BH_3 , BCl_3 , and $PdCl_2SMe_2$ are given in the Supporting Information. All compounds shown in Figures 4 and 5 are identified as minima on the potential energy hypersurface, except for **3RuC**– $W(CO)_5$, **4RuC**– $W(CO)_5$, and **4RuC**– $PdCl_2SMe_2$ for which our computational resources did not allow one to do analytical frequency calculations in a reasonable amount of time.

The interaction of the parent compound **1RuC** with the Lewis acids $M(CO)_5$ ($M = Cr, Mo, W$) leads to C_{2v} symmetric species with a linear Ru–C–M unit and an eclipsed conformation of the ligand moieties at the donor and acceptor fragments (Figure 4).⁴⁹ The two central carbon–metal bond lengths in **1RuC**– $M(CO)_5$ differ considerably. The Ru–C bond is rather short (~ 1.690 Å), although it is somewhat longer by ~ 0.04 Å as compared to the parent system **1RuC**, which agrees with the suggestion that the **1RuC**– $M(CO)_5$ π -backdonation weakens the bond. The C–M bonds are considerably longer (1.984–2.134 Å) than the Ru–C bond. The latter values are comparable to the M–CO bond length in the corresponding $M(CO)_6$ complexes (Figure 5). Note that the metal–CO bonds of the $M(CO)_5$ fragments in **1RuC**– $M(CO)_5$ all are shorter than in the parent hexacarbonyl $M(CO)_6$ and that the trans M–CO bonds in the former complexes are slightly more shortened than the cis M–CO bonds. At the same time, the C–O bonds in the $M(CO)_5$ fragments of **1RuC**– $M(CO)_5$ are slightly longer than in $M(CO)_6$. This could be interpreted as a sign that the **1RuC**– $M(CO)_5$ π -backdonation is weaker than OC – $M(CO)_5$ π -orbital interactions. We will examine this interpretation in the bonding analysis below.

The calculated bond lengths of the iron and osmium homologues **1FeC**– $W(CO)_5$ and **1OsC**– $W(CO)_5$ indicate that the structures are not very different from the ruthenium compound **1RuC**– $W(CO)_5$ (Figure 4). The variation of the phosphine substituents PR_3 from $R = \text{methyl}$ in **1RuC**– $W(CO)_5$ to $R = \text{phenyl}$ in **3RuC**– $W(CO)_5$ and $R = \text{cyclohexyl}$ in **4RuC**– $W(CO)_5$ yields a further shortening of the trans W–CO bond,

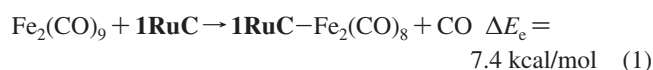
but the overall changes of the bond lengths and angles are small. Minor alterations in the calculated geometries are also observed when the halogen atom changes from chlorine in **1RuC**– $W(CO)_5$ to fluorine in **5RuC**– $W(CO)_5$, bromine in **6RuC**– $W(CO)_5$, and iodine in **7RuC**– $W(CO)_5$. The substitution of the PMe_3 phosphine ligands in **1RuC**– $W(CO)_5$ by one or two NHC ligands yielding **8RuC**– $W(CO)_5$ and **9RuC**– $W(CO)_5$ changes the bond lengths and angles of the RuC– $W(CO)_5$ moieties very little. We find in all cases that the trans W–CO bond is shorter than the cis W–CO bond and that both are still shorter than the W–CO bonds in parent $W(CO)_6$. Please note that the $[M]C$ – $M'(CO)_5$ bonds are always 0.05–0.07 Å longer than the respective OC – $M'(CO)_5$ bond.

The binding of **1RuC** to the main group Lewis acids BH_3 and BCl_3 yields C_s symmetric complexes with nearly linear Ru–C–B units (Figure 4). The boron–carbon bond in **1RuC**– BH_3 is much shorter (1.544 Å) than that in **1RuC**– BCl_3 (1.618 Å). A similar situation is found for the donor–acceptor bonds in BH_3 –CO (1.508 Å) and BCl_3 –CO (1.617 Å). The former is one of the very few stable carbonyl complexes of main group Lewis acids, whereas the latter is unstable.⁵⁰

In Figure 4, we also show the optimized structural parameters of the experimentally known complex **4RuC**– $PdCl_2SMe_2$, which are in good agreement with the experimental data, except for the Pd–C distance where the calculated value (1.915 Å) is clearly longer than the experimental data (1.853 Å).¹⁸ The difference may at least partly come from solid-state effects, which always lead to a shortening of donor–acceptor bonds.⁵⁰ The geometry of the model complex **1RuC**– $PdCl_2SMe_2$ is very similar to that of **4RuC**– $PdCl_2SMe_2$ (Figure 4).⁵¹ The calculated geometry of the carbonyl complex $PdCl_2SMe_2$ –CO exhibits very similar bond lengths and angles for the $PdCl_2SMe_2$ moiety as in **1RuC**– $PdCl_2SMe_2$ and **4RuC**– $PdCl_2SMe_2$, which agrees with the suggestion that CO and carbon complexes have similar ligand binding properties in coordination compounds.

Figure 4 gives also the optimized geometries of the porphyrin carbon complexes **10MC**– $W(CO)_5$ ($M = Fe, Ru, Os$). The latter species show a distinct influence of the group-8 atom on the C–W and W–CO bond lengths. The former bond becomes clearly longer in **10MC**– $W(CO)_5$ with $M = Fe$ (2.070 Å) < Ru (2.097 Å) < Os (2.110 Å), while the trans W–CO bonds become shorter with $M = Fe$ (2.075 Å) > Ru (2.063 Å) > Os (2.059 Å). The complex **10FeC**– $W(CO)_5$ is the only example in our series of compounds where the $[M]C$ – $M(CO)_5$ bond is shorter than the trans M–CO bond. All other complexes have metal–CO bonds that are shorter than the metal–C bonds.

Finally, we show in Figure 4 the theoretically predicted geometry of **1RuC**– $Fe_2(CO)_8$ where the carbon complex **1RuC** is bridging the iron atoms of $Fe_2(CO)_8$. The former structure is a minimum on the PES, which indicates that carbon complexes are capable like CO to serve as bridging ligands. A comparison of the geometry of **1RuC**– $Fe_2(CO)_8$ with that of $Fe_2(CO)_9$ (Figure 5) shows that the bond lengths in the $Fe_2(CO)_8$ fragments of the compounds change very little when CO is substituted by **1RuC**. The Fe–Fe distance in the carbon complex is slightly larger (2.546 Å) than that in $Fe_2(CO)_9$ (2.521 Å), but otherwise the Fe–CO and C–O distances are hardly altered. We calculated the reaction energy for the substitution of CO by **1RuC** at BP86/TZ2P:



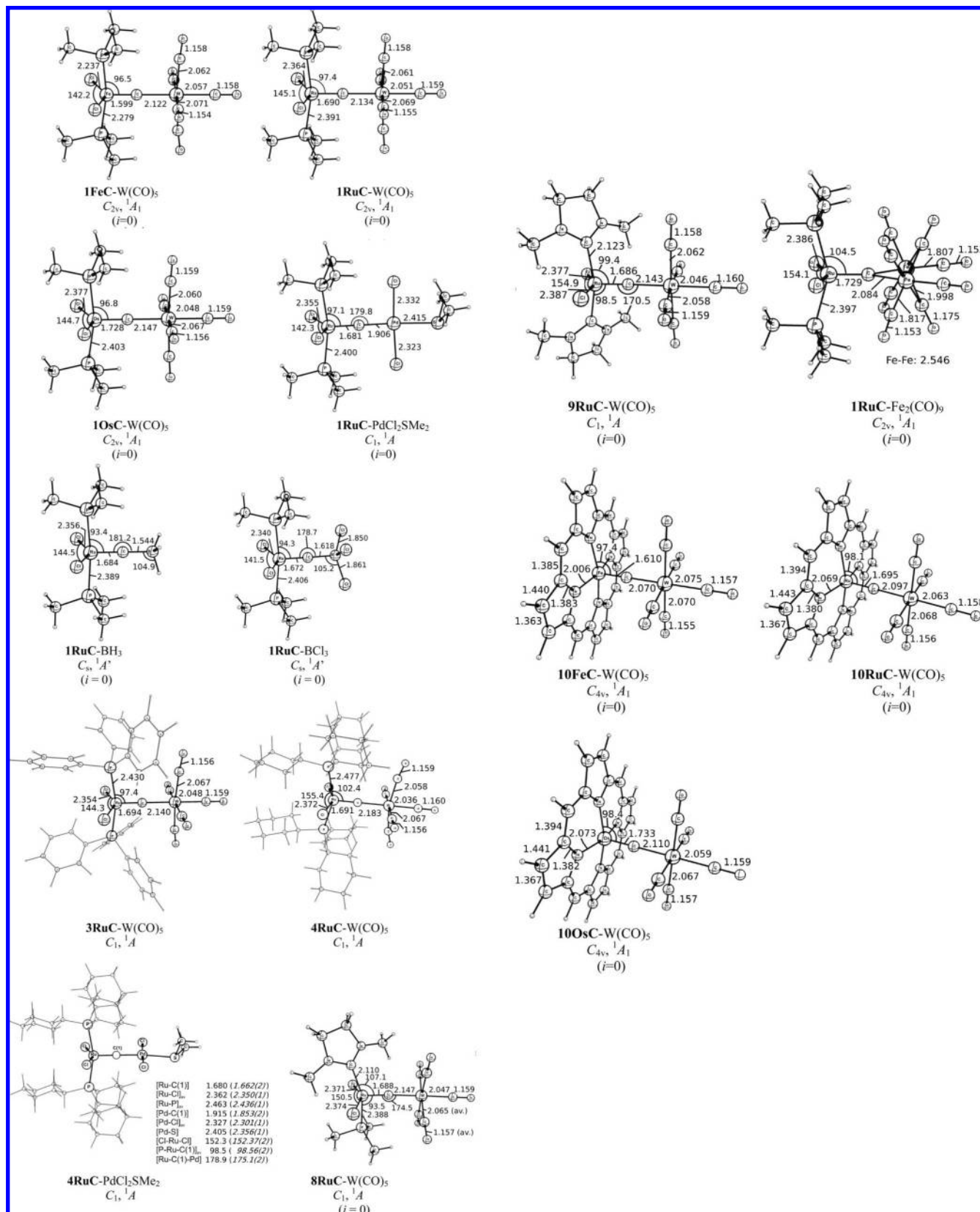


Figure 4. Optimized geometries (BP86/TZVPP) of adducts with carbon complexes as ligands. Donor–acceptor complexes of **1FeC**, **1RuC**, **1OsC**, **3RuC**, **4RuC**, **8RuC**, **9RuC**, **10FeC**, **10RuC**, and **10OsC** with W(CO)₅. Donor–acceptor complexes of **1RuC** with PdCl₂SMe₂, BH₃, BCl₃, and Fe₂(CO)₈. Donor–acceptor complex of **4RuC** with PdCl₂SMe₂. The donor–acceptor complexes **1RuC**–Cr(CO)₅, **1RuC**–Mo(CO)₅, **5RuC**–W(CO)₅, **6RuC**–W(CO)₅, and **7RuC**–W(CO)₅ are shown in the Supporting Information. In the complexes of **3RuC** and **4RuC**, the phosphine substituents are drawn with fine gray lines for reasons of clarity. Distances in Å, angles in deg. Experimental values are given in italics. Experimental data (X-ray) for **4RuC**–PdCl₂SMe₂ from ref 18.

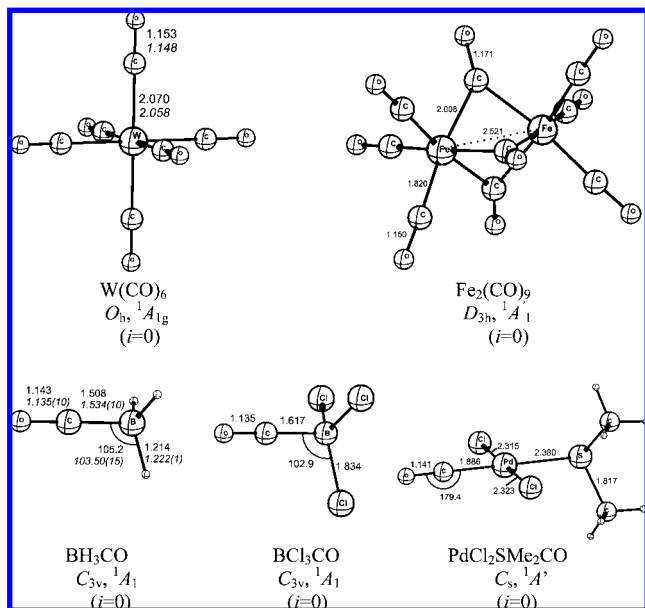


Figure 5. Optimized geometries (BP86/TZVPP) of adducts with CO as ligands. Donor–acceptor complexes of CO with $W(CO)_6$, $Fe_2(CO)_9$, BH_3 , BCl_3 , and $PdCl_2SMe_2$. The CO complexes with $Cr(CO)_5$ and $Mo(CO)_5$ are shown in the Supporting Information. Distances in Å, angles in deg. Experimental values are given in italics. Experimental data (X-ray) for $M(CO)_6$ from ref 65. Experimental data (microwave spectroscopy) for BH_3CO from ref 66.

The calculations suggest that the bridging **1RuC** ligand in **1RuC**– $Fe_2(CO)_8$ is 7.4 kcal/mol less strongly bonded than CO is in $Fe_2(CO)_9$ (6.4 kcal/mol after ZPE corrections).

Table 2 gives the calculated bond dissociation energies for the complexes of the ligands **NM**–C and CO with main group and transition metal Lewis acids. The values for **SC**– $W(CO)_5$ and **FB**– $W(CO)_5$ have also been calculated for comparison.

The first dissociation energies for the hexacarbonyl complexes $M(CO)_6$ are experimentally known.⁵² Our DFT and CCSD(T) values (Table 2) are in very good agreement with the experimental gas-phase data except for $Cr(CO)_6$, which is calculated to have a slightly higher bond dissociation energy (BDE) than experimentally found. Because of this deviation, the trend in the dissociation energies changes from $Cr(CO)_6 < Mo(CO)_6 < W(CO)_6$ in the experimental data to $Mo(CO)_6 < Cr(CO)_6 < W(CO)_6$ in the theoretical values. This discrepancy was already noted before,^{53–55} and it might be that the experimental value for the first dissociation energy of $Cr(CO)_6$ is erroneous (see discussion in ref 54). For the purpose of the current work, the most important point, however, is the very good performance of the DFT method in comparison to the ab initio calculations for $M(CO)_6$ ($M = Cr, Mo, W$). The difference in the dissociation energies is in all cases less than 1 kcal/mol.

For the main group donor–acceptor compound H_3BCO , the CCSD(T) value of 20.6 kcal/mol (D_0) is in reasonable agreement with the experimental value of 24.6 kcal/mol and with previous theoretical data at CCSD(T) ($D_0 = 21.1$ kcal/mol),⁵⁶ MP2 ($D_0 = 23.0$ kcal/mol),⁵⁰ and CBS-4 ($D_0 = 21.9$ kcal/mol)⁵⁷ levels, whereas our DFT calculations predict the H_3B –CO bond too stable ($D_0 = 34.6$ kcal/mol). The BP86 functional apparently overestimates the bond strength of some boron complexes, which is in agreement with the results reported by Gilbert.⁵⁸ There seems to be a systematic error in the BP86 values for BH_3 complexes, because the theoretical value for **2RuC**– BH_3 ($D_0 = 38.5$ kcal/mol) is also clearly larger than the CCSD(T)

Table 2. Calculated Bond Dissociation Energies D_0 and Reaction Enthalpies at 0 K (D_0) and at 298 K (H_{298}) at BP86/TZVPP (Denoted BP86) and CCSD(T)/TZVPP/BP86/TZVPP (Denoted CCSD(T))^a

molecule	BP86		CCSD(T)			exp.
	D_0	D_0	D_0	D_0^b	H_{298}^c	
1RuC – $Cr(CO)_5$	40.4	39.1	41.5			
2RuC – $Cr(CO)_5$	42.0	41.0	43.4	– ^f		
1RuC – $Mo(CO)_5$	38.4	37.7	40.1			
2RuC – $Mo(CO)_5$	39.6	39.0	41.4	46.1	45.5	47.9
1RuC – $W(CO)_5$	43.6	42.9	45.3			
2RuC – $W(CO)_5$	44.8	44.2	46.5	51.9	51.3	53.7
1FeC – $W(CO)_5$	43.7	43.0	45.4			
1OsC – $W(CO)_5$	45.5	44.8	47.2			
1RuC – BH_3	41.7	39.5	41.9			
2RuC – BH_3	40.4	38.5	40.9	29.9	29.0	31.4
1RuC – BCl_3	19.5	18.3	20.7			
2RuC – BCl_3	14.7	13.8	16.2	14.2	13.3	15.7
1RuC – $PdCl_2SMe_2$	45.4	44.1	46.5			
3RuC – $W(CO)_5$	37.7	– ^g				
4RuC – $W(CO)_5$	33.8	– ^g				
4RuC – $PdCl_2SMe_2$	37.7	– ^g				
5RuC – $W(CO)_5$	45.3	44.5	46.9			
6RuC – $W(CO)_5$	43.0	42.4	44.8			
7RuC – $W(CO)_5$	42.4	41.8	44.2			
8RuC – $W(CO)_5$	41.3	40.5	42.9			
9RuC – $W(CO)_5$	39.7	38.8	41.2			
10FeC – $W(CO)_5$	51.0	50.2	52.6			
10RuC – $W(CO)_5$	50.0	49.0	51.4			
10OsC – $W(CO)_5$	51.7	51.0	53.4			
OC– $Cr(CO)_5$	42.5	40.1	42.2	42.3	39.9	36.8±2 ^d
OC– $Mo(CO)_5$	39.9	37.9	40.0	39.0	37.0	40.5±2 ^d
OC– $W(CO)_5$	44.5	42.5	44.6	43.8	41.8	46.0±2 ^d
OC– BCl_3	0.1	<0.0	2.1	–5.5	–5.6	–3.5
OC– BH_3	37.8	34.6	36.7	23.8	20.6	24.6 ^e
OC– $PdCl_2SMe_2$	34.0	32.0	34.4			
SC– $W(CO)_5$	62.0	60.4	62.8			
FB– $W(CO)_5$	60.6	58.8	61.2			

^a Energies in kcal/mol. ^b Zero-point vibrational correction from the BP86/TZVPP calculations. ^c The empirical thermal correction to D_0 amounts to $1/2RT$ per rotational or translational degree of freedom and to RT for the work term pV . This amounts to –2.1 kcal/mol for the hexacarbonyl complexes and to –2.4 kcal/mol for the other molecules.

^d Gas-phase values based on pulsed laser pyrolysis, ref 52.

^e Experimental value taken from the heats of formation, ref 67. ^f No SCF convergence. ^g Analytical frequency calculations too large for the available computational resources.

value ($D_0 = 29.0$ kcal/mol). The differences between the BP86 and CCSD(T) values are much smaller for the BCl_3 complexes. Table 2 shows that the calculated bond energies for **2RuC**– BCl_3 ($D_0 = 13.8$ kcal/mol at BP86 and $D_0 = 13.3$ kcal/mol at CCSD(T)) agree quite well. The complex Cl_3BCO has a very long B–C bond, which has a negligible BDE at BP86. The molecule is even unbound at CCSD(T).

Table 2 shows that the donor–acceptor bonds between the carbon complexes and Lewis acids possess dissociation energies similar to those of the CO complexes. Please note that the D_0 values at BP86 for the adducts of $M(CO)_5$ with the parent carbon complex **1RuC** and with CO are almost the same. The CCSD(T) data for the complexes of **2RuC** with $M(CO)_5$ indicate that BP86 slightly underestimates the strength of the donor–acceptor bond by about 6–7 kcal/mol (Table 2). The main-group Lewis acid BH_3 also binds quite strongly to the $[L_4M(C)]$ complexes, but BP86 overestimates the stability by ~10 kcal/mol. Nevertheless, with a binding energy of ~30 kcal/mol, the BH_3 complexes of the carbon compounds should be sufficiently stable to become isolated experimentally. BCl_3 forms much longer and much weaker bonds to the carbon complexes than does BH_3 , but, unlike Cl_3BCO , complexes $[TM]C$ – BCl_3 might be stable

enough to become synthesized. The calculated BDEs of **1RuC**– BCl_3 and **2RuC**– BCl_3 should be sufficient to isolate the compounds.

Table 2 shows that the BDE of **1RuC**– $\text{PdCl}_2\text{SMe}_2$ ($D_0 = 44.1$ kcal/mol) is nearly the same as that of **1RuC**– $\text{W}(\text{CO})_5$ ($D_0 = 42.9$ kcal/mol). The BDE of the experimentally known¹⁸ complex **4RuC**– $\text{PdCl}_2\text{SMe}_2$ is ~ 7 kcal/mol lower than that of **1RuC**– $\text{PdCl}_2\text{SMe}_2$. The calculated values are important for the interpretation of experimental findings. Grubbs reported¹⁸ that the complex **4RuC**– $\text{Mo}(\text{CO})_5$ was synthesized and was identified by its NMR spectrum but it could not become isolated. Because $\text{Mo}(\text{CO})_5$ binds ~ 5 kcal/mol less strongly to carbon complexes than does $\text{W}(\text{CO})_5$ (Table 2), it might be worthwhile to use tungsten carbonyls instead of molybdenum carbonyls in the experiments.

We want to point out that the BDE of **1RuC**– $\text{PdCl}_2\text{SMe}_2$ is 8 kcal/mol higher than the BDE of OC – $\text{PdCl}_2\text{SMe}_2$ ($D_0 = 32.0$ kcal/mol), while the BDEs of the metal–carbon pentacarbonyl complexes **NMC**– $\text{M}(\text{CO})_5$ are similar or slightly lower than the related OC – $\text{M}(\text{CO})_5$ bond energies (Table 2). Even the BDE of the isolated complex **4RuC**– $\text{PdCl}_2\text{SMe}_2$ ($D_e = 37.7$ kcal/mol), which has bulky phosphine substituents, is slightly higher than the BDE of OC – $\text{PdCl}_2\text{SMe}_2$ ($D_e = 34.0$ kcal/mol). This finding explains why the complex **4RuC**– $\text{PdCl}_2\text{SMe}_2$ could become isolated and characterized by X-ray structure analysis, while the complex $[\text{Cl}_2(\text{PCyc}_3)_2\text{Ru}(\text{C})]$ – $\text{Mo}(\text{CO})_5$ could only become identified via its NMR spectrum but it could not become isolated so far.¹⁸ The calculated bond strengths suggest that complexes of d^{10} transition metals (which are formally d^8 in the oxidation state +2) with metal carbon complexes as ligands might be more stable than complexes of d^6 elements.

Changing the ligand and the central metal in the carbon fragments $[\text{L}_4\text{M}(\text{C})]$ of the complexes with $\text{M}'(\text{CO})_5$ changes the BDE of the L_4MC – $\text{M}'(\text{CO})_5$ bond only slightly. The NHC ligands in **8RuC**– $\text{W}(\text{CO})_5$ and **9RuC**– $\text{W}(\text{CO})_5$ weaken the bond a bit. Changing the halogen atoms in **XRuC**– $\text{W}(\text{CO})_5$ weakens the bond with the trend $\text{F} > \text{Cl} > \text{Br} > \text{I}$. A clearly stronger $[\text{TM}]\text{C}$ – $\text{W}(\text{CO})_5$ bond is calculated for the porphyrin carbon complexes **10MC**– $\text{W}(\text{CO})_5$, which have BDEs between $D_0 = 49.0$ – 51.0 kcal/mol (Table 2). Note that the trend of the BDE is opposite to what could be expected from the bond lengths. Complex **10OsC**– $\text{W}(\text{CO})_5$ has clearly the longest bond but the highest BDE of the three compounds.

We also calculated the structures and BDEs of the series of tungsten complexes $\text{W}(\text{CO})_n(\mathbf{2RuC})_{6-n}$ with $n = 0$ – 5 where the CO ligands of $\text{W}(\text{CO})_6$ are successively substituted by the carbon complex $[\text{RuCl}_2(\text{PH}_3)_2(\text{C})]$ (**2RuC**). We have chosen **2RuC** as the metal carbon ligand because the size of the complexes makes it impossible for us to use **1RuC** as ligand. Figure 6 shows the optimized geometries of $\text{W}(\text{CO})_n(\mathbf{2RuC})_{6-n}$.

The **2RuC**– $\text{W}(\text{CO})_5$ bond of the mono carbon complex $\text{W}(\text{CO})_5(\mathbf{2RuC})$ is slightly shorter (2.095 Å) than the **1RuC**– $\text{W}(\text{CO})_5$ bond (2.134 Å; Figure 4), but geometries are otherwise very similar. The trans isomer of the disubstituted carbon complex $\text{W}(\text{CO})_4(\mathbf{2RuC})_2$ is 3.1 kcal/mol higher in energy than that of *cis*- $\text{W}(\text{CO})_4(\mathbf{2RuC})_2$ (Figure 6). The **2RuC**– W bonds in both isomers are shorter than that in $\text{W}(\text{CO})_5(\mathbf{2RuC})$. Note that *trans*- $\text{W}(\text{CO})_4(\mathbf{2RuC})_2$ has shorter **2RuC**– W bonds than does *cis*- $\text{W}(\text{CO})_4(\mathbf{2RuC})_2$. The same situation is observed for the trisubstituted carbon complex $\text{W}(\text{CO})_3(\mathbf{2RuC})_3$, where the **2RuC**– W bonds that are trans to each other are shorter than **2RuC**– W bonds that are trans to CO. The *mer*- $\text{W}(\text{CO})_3(\mathbf{2RuC})_3$ isomer is 4.3 kcal/mol more

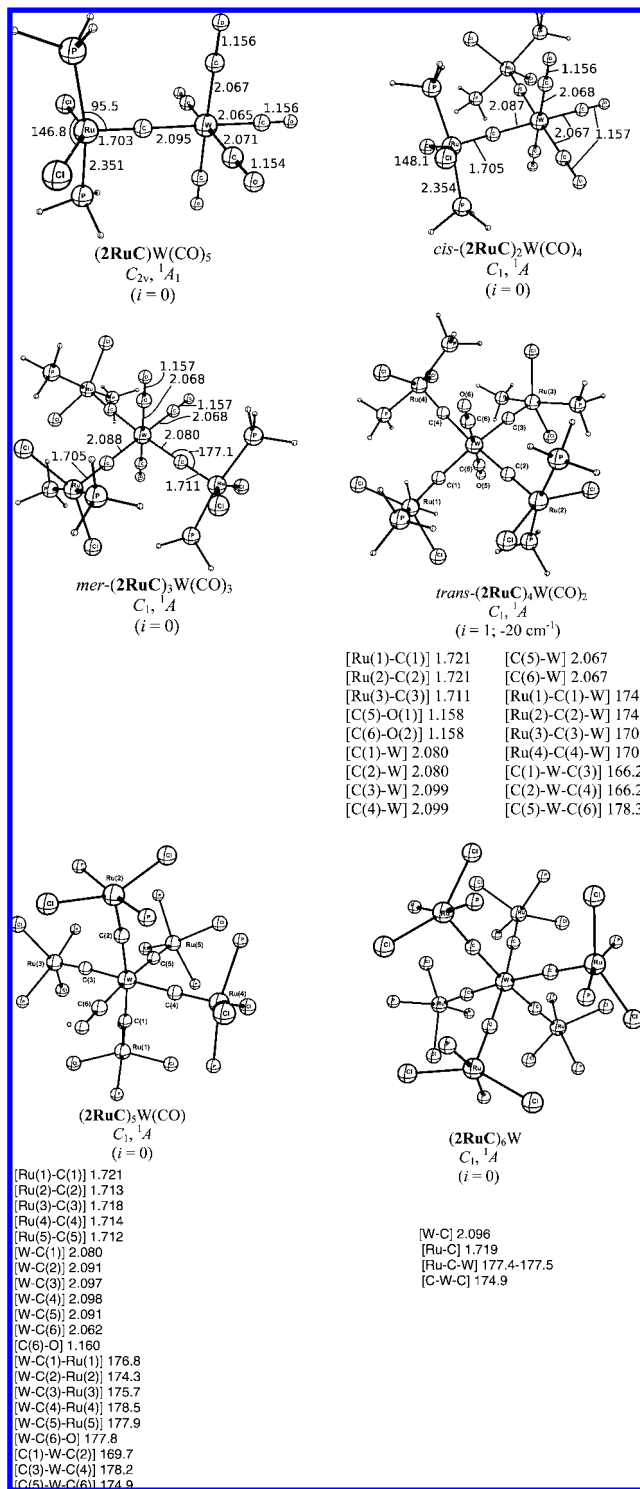


Figure 6. Optimized geometries (BP86/TZVPP) of the complexes $(\mathbf{2RuC})_n\text{W}(\text{CO})_{6-n}$ ($n = 1$ – 6). Distances in Å, angles in deg. The structures of the energetically higher lying isomers *trans*- $(\mathbf{2RuC})_2\text{W}(\text{CO})_4$, *fac*- $(\mathbf{2RuC})_3\text{W}(\text{CO})_3$, and *cis*- $(\mathbf{2RuC})_4\text{W}(\text{CO})_2$ are shown in the Supporting Information. Relative energies E_{rel} of the isomers are given in kcal/mol. In $(\mathbf{2RuC})_5\text{W}(\text{CO})$ and $(\mathbf{2RuC})_6\text{W}$, we omitted the hydrogen atoms of the PH_3 groups for clarity.

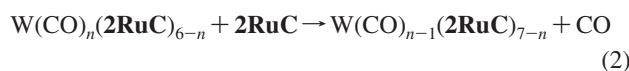
stable than *fac*- $\text{W}(\text{CO})_3(\mathbf{2RuC})_3$. For the complexes with four **2RuC** ligands, the calculations predict that *trans*- $\text{W}(\text{CO})_2(\mathbf{2RuC})_4$ is 6.3 kcal/mol lower in energy than is *cis*- $\text{W}(\text{CO})_2(\mathbf{2RuC})_4$. The calculation of the vibrational frequencies of *trans*- $\text{W}(\text{CO})_2(\mathbf{2RuC})_4$, *trans*- $\text{W}(\text{CO})_4(\mathbf{2RuC})_2$, and *fac*-

Table 3. Calculated Reaction Energies ΔE_e and Reaction Enthalpies (0 K) ΔE_0 at BP86/TZVPP in kcal/mol

reaction	ΔE_e	ΔE_0
$W(CO)_6 + 2RuC \rightarrow W(CO)_5(2RuC) + CO$	-0.3	-1.7
$W(CO)_5(2RuC) + 2RuC \rightarrow W(CO)_4(2RuC)_2 + CO$	-4.2	-5.5
$W(CO)_4(2RuC)_2 + 2RuC \rightarrow W(CO)_3(2RuC)_3 + CO$	-4.8	-6.2
$W(CO)_3(2RuC)_3 + 2RuC \rightarrow W(CO)_2(2RuC)_4 + CO$	-2.0	-3.5
$W(CO)_2(2RuC)_4 + 2RuC \rightarrow W(CO)(2RuC)_5 + CO$	6.7	6.2
$W(CO)(2RuC)_5 + 2RuC \rightarrow W(2RuC)_6 + CO$	0.4	-0.4

$W(CO)_3(2RuC)_3$ gave one imaginary frequency, which comes from a spurious energy maximum for rotation of the phosphine ligands that can be neglected. The penta- and hexasubstituted systems $W(CO)(2RuC)_5$ and $W(2RuC)_6$ show the expected geometries. Note that the $2RuC$ – W bonds in the homoleptic complex $W(2RuC)_6$ are slightly longer than that in $W(CO)_5(2RuC)$.

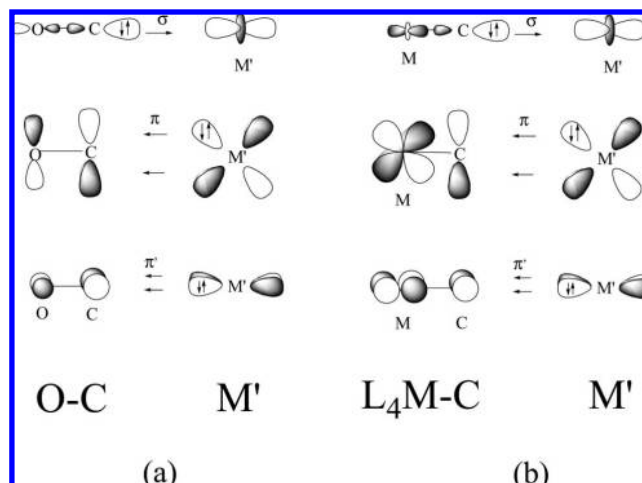
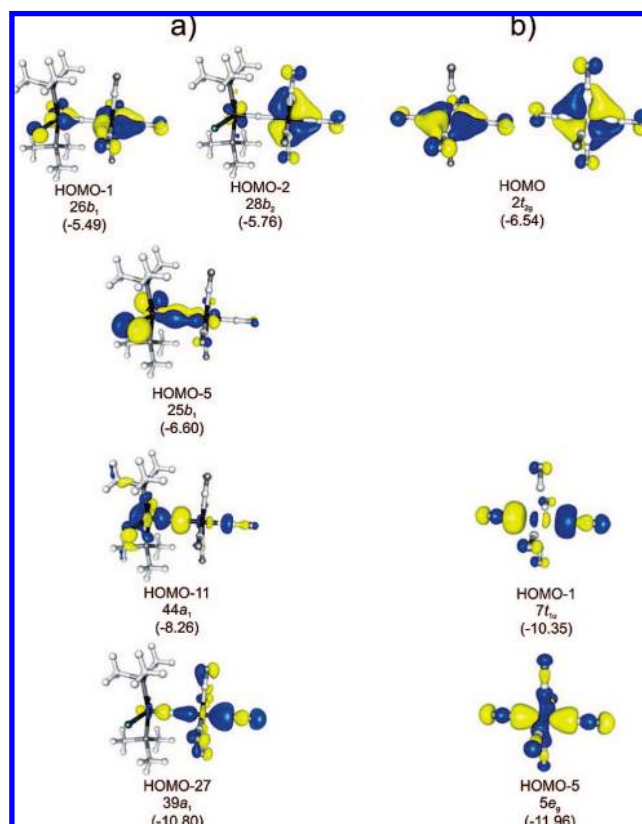
Table 3 gives the theoretically predicted differences between the BDEs of CO and $2RuC$ in $W(CO)_n(2RuC)_{6-n}$, which are calculated using the energies of the ligand substitution reaction 2:



The data in Table 3 suggest that the successive substitution of OC in $W(CO)_6$ by $2RuC$ is always slightly exothermic except for the formation of the penta-coordinated carbon complex $W(CO)(2RuC)_5$. The sum of the reaction energies of reaction 2 gives a value of $D_0 = -11.1$ kcal/mol. This means that the formation of the homoleptic carbon complex $W(2RuC)_6$ from $W(CO)_6$ is a thermodynamically favored reaction. We want to point out that the bond energy of the methyl substituted homologue $1RuC$ – $W(CO)_5$ is slightly lower than the bond energy of $2RuC$ – $W(CO)_5$ (Table 2). It is possible that the analogous reaction energies of reaction 2 for $W(CO)_n(1RuC)_{6-n}$ might be less exothermic or endothermic as compared to the reactions of $W(CO)_n(2RuC)_{6-n}$.

Analysis of the Bonding Situation. The donor–acceptor bonding of CO as ligand to a transition metal is usually discussed using the familiar Dewar–Chatt–Duncanson model.^{7–9} A very similar bonding scenario with σ -donation and π -backdonation between a ligand and a metal can also be sketched for metal carbon complexes. This is qualitatively shown in Figure 7.

Visual inspection of the valence orbitals show a great similarity between the $1RuC$ – $W(CO)_5$ and OC – $W(CO)_5$ bonding region. Figure 8 displays the actual Kohn–Sham orbitals of $1RuC$ – $W(CO)_5$ and $W(CO)_6$, which are relevant for the discussion. The HOMO–5 ($5e_g$) and the HOMO–1 ($7t_{1u}$) of $W(CO)_6$ are OC – W σ -bonding and σ -antibonding orbitals, respectively. The analogous orbitals of $1RuC$ – $W(CO)_5$ are the HOMO–27 ($39a_1$) and the HOMO–11 ($44a_1$). The bonding combination ($39a_1$) is polarized toward the CO group trans to the $[Cl_2(PMe_3)_2Ru(C)]$ fragment; the antibonding orbital ($44a_1$) has the larger coefficients on the $[Cl_2(PMe_3)_2Ru(C)]$ unit. The $M \rightarrow CO$ π -backdonation in $W(CO)_6$ is reflected in the HOMO ($2t_{2g}$), which results from the combination of the π^* -orbitals of CO with the metal d_{xz} , d_{yz} , and d_{xy} AOs. The analogous orbitals of $1RuC$ – $W(CO)_5$ are the HOMO–1 ($26b_1$) and the HOMO–2 ($28b_2$) MOs. A closer examination reveals that the π -backdonation in $1RuC$ – $W(CO)_5$ is a bit more complicated because it involves the π^* -antibonding orbitals HOMO–1 and HOMO–2 but also the π -bonding orbital HOMO–5 ($25b_1$) (Figure 8).

**Figure 7.** Pictorial representation of the donor–acceptor bonding between (a) CO and a transition metal compound $[M']$; and (b) a carbon complex with a terminal carbon atom $[L_4M(C)]$ and a transition metal compound $[M']$.**Figure 8.** Selected Kohn–Sham molecular orbitals of (a) $[RuCl_2-(PMe_3)_2(C)]W(CO)_5$ and (b) $W(CO)_6$ at BP86/TZVPP. Orbital energies are given in eV.

A quantitative analysis of the orbital interactions comes from charge and energy decomposition analyses. We first discuss the results of a charge decomposition analysis where we use the atomic charges and the orbital occupation from the NBO calculations. The numerical results for the complexes and the free ligands are shown in Table 4.

The carbon atom of free and bonded CO has a higher positive charge than the carbon atom of the free and bonded carbon complexes $[TM]C$, which is less positively or even slightly negatively charged. The partial charges $q(L)$ of the ligands OC

Table 4. NBO Partial Charges at BP86/TZVPP for the Complexes and Ligands L^a

molecule	$q(\text{C})$	$2s(\text{C})_{\sigma}$	$2p_z(\text{C})_{\sigma}$	$2p_x(\text{C})_{\pi}$	$2p_y(\text{C})_{\pi}$	$\Delta q(\text{C})_{\sigma}$	$\Delta q(\text{C})_{\pi}$	$q(\text{L})$
1RuC –Cr(CO) ₅	0.17	1.43	0.98	0.69	0.65	0.32	–0.15	0.29
1RuC –Mo(CO) ₅	0.07	1.47	1.02	0.71	0.65	0.24	–0.17	0.20
1RuC –W(CO) ₅	0.03	1.47	1.05	0.72	0.67	0.21	–0.20	0.17
1FeC –W(CO) ₅	0.03	1.49	1.08	0.67	0.65	0.17	–0.22	0.15
1OsC –W(CO) ₅	–0.08	1.47	1.10	0.77	0.68	0.24	–0.21	0.20
1RuC –BH ₃	0.25	1.27	0.99	0.73	0.72	0.47	–0.26	0.43
1RuC –BCl ₃	0.15	1.32	0.98	0.73	0.76	0.43	–0.30	0.51
5RuC –W(CO) ₅	–0.01	1.48	1.05	0.77	0.67	0.23	–0.19	0.21
6RuC –W(CO) ₅	0.02	1.47	1.05	0.72	0.67	0.21	–0.21	0.16
7RuC –W(CO) ₅	0.00	1.47	1.06	0.73	0.68	0.19	–0.23	0.15
10FeC –W(CO) ₅	0.19	1.49	1.05	0.61	0.61	0.21	–0.26	0.09
10RuC –W(CO) ₅	0.13	1.46	1.05	0.65	0.65	0.26	–0.22	0.14
10OsC –W(CO) ₅	0.02	1.46	1.08	0.70	0.70	0.28	–0.22	0.17
OC–Cr(CO) ₅	0.69	1.20	0.81	0.62	0.62	0.54	–0.30	0.28
OC–Mo(CO) ₅	0.59	1.25	0.86	0.63	0.63	0.44	–0.32	0.18
OC–W(CO) ₅	0.54	1.25	0.87	0.65	0.65	0.43	–0.36	0.13
OC–BH ₃	0.75	1.07	0.84	0.65	0.65	0.64	–0.36	0.39
OC–BCl ₃	0.70	1.13	0.85	0.64	0.64	0.57	–0.34	0.38
Ligand L								
1RuC	0.06	1.81	0.92	0.65	0.54			
1FeC	0.12	1.82	0.92	0.57	0.53			
1OsC	–0.07	1.81	1.00	0.69	0.55			
5RuC	–0.02	1.83	0.93	0.71	0.54			
6RuC	0.07	1.81	0.92	0.64	0.54			
7RuC	0.07	1.80	0.92	0.64	0.54			
10FeC	0.27	1.85	0.90	0.48	0.48			
10RuC	0.13	1.83	0.94	0.54	0.54			
10OsC	–0.01	1.84	0.98	0.59	0.59			
OC	0.46	1.66	0.89	0.47	0.47			

^a $q(\text{C})$ gives the partial charge at the carbon donor atom. $2s(\text{C})-2p_z(\text{C})$ are the occupation numbers of the Natural Atomic Orbitals (NAOs). $\Delta q(\text{C})_{\sigma}$ and $\Delta q(\text{C})_{\pi}$ give the change in the $p(\sigma)$ and $p(\pi)$ occupation of the carbon donor atoms with respect to the free ligands. $q(\text{L})$ gives the partial charge of the ligands.

and [TM]C in the complexes indicate that the net charge transfer between L and the Lewis acid for the two classes of donor ligands is very similar. The calculated values $q(\text{L})$ for **1RuC**–M(CO)₅ and OC–M(CO)₅ (M = Cr, Mo, W) are nearly the same. Larger positive charges are likewise calculated for the CO and **1RuC** complexes of BH₃ and BCl₃ (Table 4). A more detailed insight into the charge reorganization that is brought about by the complex formation comes from the orbital charges. Table 4 shows that the L→M(CO)₅ σ -donation comes mainly from the 2s orbital of the carbon donor atom in OC and [TM]C, while the occupation of the 2p(σ) AO changes much less. The occupation of the p(π) AOs at the carbon atoms increases, which is due to the L←M(CO)₅ π -backdonation. According to the NBO data, the [TM]C→M(CO)₅ σ -donation $\Delta q(\text{C})_{\sigma}$ has strength similar to that of the [TM]C←M(CO)₅ π -backdonation $\Delta q(\text{C})_{\pi}$, and the latter may even be slightly larger than the former. The overall partial charge of the ligand is always positive, however, which is not consistent with the calculated values for $q(\text{L})$. The difference comes from the fact that the NBO algorithm for assigning charges to fragments yields so-called Rydberg orbitals, which are neglected when only the charges of the valence orbitals are considered. The Rydberg orbitals play a larger role for the bigger ligands [TM]C than for OC. Therefore, the difference between the L→M(CO)₅ σ -donation and the L←M(CO)₅ π -backdonation deviates less from $q(\text{L})$ when L = CO than for L = [TM]C. Note that the absolute values for the σ -donation $\Delta q(\text{C})_{\sigma}$ and π -backdonation $\Delta q(\text{C})_{\pi}$ of OC are larger than that for [TM]C, which comes from the shorter metal–ligand bonds of the former ligand as compared to the latter.

More comprehensive information about the behavior of [TM]C and OC as ligands is given by the EDA results, which provide not only quantitative information about the strength of L→M(CO)₅ σ -donation and L←M(CO)₅ π -backdonation in terms of energy contributions. The data make it also possible to estimate the electrostatic contributions to the metal–ligand binding, which is totally neglected when only the DCD bonding model is considered.⁷¹ Table 5 gives the EDA results for the bonding interactions in **1RuC**–M(CO)₅ (M = Cr, Mo, W), **1RuC**–BH₃, and **1RuC**–BCl₃. The data for the OC complexes OC–M(CO)₅, OC–BH₃, and OC–BCl₃ are given in Table 6.

The EDA results show that the relative and even the absolute contributions of the electrostatic bonding ΔE_{elstat} and the orbital (covalent) bonding ΔE_{orb} of the ligands **1RuC** and OC have very similar values. This holds for the transition metal carbonyl complexes L–M(CO)₅ where the orbital term contributes between 46% and 48% to the total attractive interactions, as well as for the complexes L–BH₃ and L–BCl₃ where ΔE_{orb} is clearly stronger than ΔE_{elstat} . The breakdown of ΔE_{orb} into contributions from orbitals possessing different symmetry clearly shows that OC is a weaker σ -donor and a stronger π -acceptor than **1RuC**. Figure 2 shows that the σ -donor orbitals of **1RuC** (HOMO–3 and HOMO–6) are much higher in energy than the σ -donor orbitals of OC (HOMO and HOMO–2) and that the π -acceptor orbitals of **1RuC** (LUMO+1 and LUMO+2) are higher in energy than the degenerate π -acceptor orbital of OC (LUMO).⁷⁷ The relative and absolute contributions of $\Delta E(\sigma)$ [$\Delta E(\pi)$] to ΔE_{orb} in the OC complexes (Table 6) are clearly smaller [larger] than those in the **1RuC** complexes (Table 5). This is in agreement with the suggestion that was made in the discussion about the calculated bond lengths (see above). Note that the energy contribution from $\Delta E a''(\pi)$ in **1RuC**–BH₃ and **1RuC**–BCl₃ gives only one component of the total π -bonding. The molecules have C_s symmetry, and thus only contributions from a' and a'' orbitals can be distinguished. However, the data for the $\Delta E b_1(\pi)$ and $\Delta E b_2(\pi)$ contributions to the total π -bonding in **1RuC**–M(CO)₅ (Table 5) show that the strengths of the π -orbital interactions in the two planes are very similar to each other. It can therefore be assumed that the total π -bonding in **1RuC**–BH₃ and **1RuC**–BCl₃ is about twice as strong as the value calculated for $\Delta E a''(\pi)$.

Table 7 gives the EDA results for the group-8 complexes **1MC**–W(CO)₅ and **10MC**–W(CO)₅ (M = Fe, Ru, Os). The bond dissociation energy of the porphyrin metal–carbon ligands in **10MC**–W(CO)₅ is slightly stronger than the BDE of the ligands **1MC** in **1MC**–W(CO)₅. The nature of the bonding is very similar, which can be seen from the percentage contributions of the electrostatic and orbital terms. The EDA results suggest that the π -backdonation in **10MC**–W(CO)₅ makes a larger percentage contribution to ΔE_{orb} than in **1MC**–W(CO)₅. Table 8 gives the EDA results for the halogen systems **NRuC**–W(CO)₅ with fluorine (N = 5), chlorine (N = 1), bromine (N = 6), and iodine (N = 7). The nature of the bonding changes only slightly. Note that the calculated bond dissociation energy deceptively suggests that the **NRuC**–W(CO)₅ interactions in the fluorine compound **5RuC**–W(CO)₅ are weaker than in the other compounds. The lower D_e value of the latter compound

(77) One referee pointed out that the energy difference between the π -acceptor orbitals of **1RuC** and CO is much smaller than the energy difference between the σ -donor orbitals of the two ligands. We want to point out that the energy of a vacant orbital is calculated in the SCF converged field of the occupied orbitals and that the energy levels of vacant orbitals tend to be much closer to each other than do those of occupied orbitals.

Table 5. Energy Decomposition Analysis of the **1RuC**–M(CO)₅ (M = Cr, Mo, W) Bond in C_{2v} Symmetry and of the **1RuC**–BX₃ (X = H, Cl) Bond in C_s Symmetry at BP86/TZ2P//BP86/TZVPP^a

	1RuC –Cr(CO) ₅	1RuC –Mo(CO) ₅	1RuC –W(CO) ₅	1RuC –BH ₃	1RuC –BCl ₃
ΔE_{int}	–43.9	–41.8	–49.7	–58.2	–45.3
ΔE_{Pauli}	101.7	96.5	110.0	142.8	203.6
$\Delta E_{\text{Elstat}}^b$	–74.5 (51.2%)	–73.2 (52.9%)	–85.8 (53.7%)	–67.3 (33.5%)	–99.9 (40.1%)
ΔE_{Orb}^b	–71.1 (48.8%)	–65.1 (47.1%)	–73.9 (46.3%)	–133.7 (66.5%)	–149.0 (59.9%)
$\Delta E_{a_1(\sigma)}^c$	–44.6 (62.7%)	–39.9 (61.3%)	–45.8 (62.0%)		
$\Delta E_{a_2(\delta)}^c$	–0.3 (0.4%)	–0.3 (0.5%)	–0.3 (0.4%)		
$\Delta E_{b_1(\pi)}^c$	–12.3 (17.3%)	–11.7 (17.9%)	–13.1 (17.7%)		
$\Delta E_{b_2(\pi)}^c$	–13.9 (19.6%)	–13.2 (20.3%)	–14.7 (19.9%)		
$\Delta E_{a'}(\sigma+\pi)^c$				–122.0 (91.2%)	–139.0 (93.3%)
$\Delta E_{a''}(\pi)^c$				–11.7 (8.8%)	–10.0 (6.7%)
ΔE_{Prep}	2.3	3.0	4.3	11.1	31.8
$\Delta E (= -D_e)$	–41.6	–38.9	–45.3	–47.0	–13.5

^a Energies in kcal/mol. ^b Values in parentheses give the percentage contribution to the total attractive interaction ($\Delta E_{\text{Elstat}} + \Delta E_{\text{Orb}}$). ^c Values in parentheses give the percentage contribution to the total orbital interaction (ΔE_{Orb}).

Table 6. Energy Decomposition Analysis of the OC–M(CO)₅ (M = Cr, Mo, W) Bond in C_{4v} Symmetry and of the OC–BX₃ (X = H, Cl) Bond in C_{3v} Symmetry at BP86/TZ2P//BP86/TZVPP^a

	OC–Cr(CO) ₅	OC–Mo(CO) ₅	OC–W(CO) ₅	OC–BH ₃	OC–BCl ₃
ΔE_{int}	–45.1	–43.1	–49.7	–50.3	–15.4
ΔE_{Pauli}	109.1	102.1	118.6	152.0	208.8
$\Delta E_{\text{Elstat}}^b$	–78.9 (51.2%)	–75.1 (51.8%)	–89.7 (53.3%)	–74.0 (36.6%)	–97.1 (43.3%)
ΔE_{Orb}^b	–75.3 (48.8%)	–70.0 (48.2%)	–78.6 (46.7%)	–128.4 (63.4%)	–127.2 (56.7%)
$\Delta E_{a_1(\sigma)}^c$	–34.9 (46.3%)	–31.8 (45.4%)	–36.3 (46.1%)		
$\Delta E_{a_2}^c$	0.0 (0.0%)	0.0 (0.0%)	0.0 (0.0%)		
$\Delta E_{b_1}^c$	–0.1 (0.1%)	0.0 (0.0%)	0.0 (0.0%)		
$\Delta E_{b_2}^c$	0.0 (0.1%)	0.0 (0.1%)	0.0 (0.0%)		
$\Delta E_{e(\pi)}^c$	–40.3 (53.5%)	–38.2 (54.6%)	–42.3 (53.9%)		
$\Delta E_{a_1(\sigma)}^c$				–91.1 (71.0%)	–102.0 (80.2%)
$\Delta E_{a_2(\delta)}^c$				0.0 (0.0%)	–0.1 (0.1%)
$\Delta E_{e(\pi)}^c$				–37.3 (29.0%)	–25.1 (19.7%)
ΔE_{Prep}	8.3	7.8	9.4	7.7	22.2
$\Delta E (= -D_e)$	–43.2	–39.6	–45.7	–42.6	6.8

^a Energies in kcal/mol. ^b Values in parentheses give the percentage contribution to the total attractive interaction ($\Delta E_{\text{Elstat}} + \Delta E_{\text{Orb}}$). ^c Values in parentheses give the percentage contribution to the total orbital interaction (ΔE_{Orb}).

Table 7. Energy Decomposition Analysis of the **1MC**–W(CO)₅ (M = Fe, Ru, Os) Bond in C_{2v} Symmetry and of the **10MC**–W(CO)₅ (M = Fe, Ru, Os) Bond in C_{4v} Symmetry at BP86/TZ2P//BP86/TZVPP^a

	1FeC –W(CO) ₅	1RuC –W(CO) ₅	1OsC –W(CO) ₅	10FeC –W(CO) ₅	10RuC –W(CO) ₅	10OsC –W(CO) ₅
ΔE_{int}	–50.9	–49.7	–51.1	–57.9	–56.2	–57.8
ΔE_{Pauli}	116.8	110.0	112.2	135.4	128.7	125.6
$\Delta E_{\text{Elstat}}^b$	–89.1 (53.1%)	–85.8 (53.7%)	–92.2 (56.5%)	–99.4 (51.4%)	–99.2 (53.7%)	–103.9 (56.6%)
ΔE_{Orb}^b	–78.6 (46.9%)	–73.9 (46.3%)	–71.1 (43.5%)	–93.8 (48.6%)	–85.6 (46.3%)	–79.5 (43.4%)
$\Delta E_{a_1(\sigma)}^c$	–49.2 (62.6%)	–45.8 (62.0%)	–45.5 (63.9%)			
$\Delta E_{a_2(\delta)}^c$	–0.3 (0.3%)	–0.3 (0.4%)	–0.3 (0.4%)			
$\Delta E_{b_1(\pi)}^c$	–14.0 (17.8%)	–13.1 (17.7%)	–11.7 (16.5%)			
$\Delta E_{b_2(\pi)}^c$	–15.1 (19.3%)	–14.7 (19.9%)	–13.7 (19.2%)			
$\Delta E_{a_1(\sigma)}^c$				–53.3 (56.8%)	–49.3 (57.5%)	–48.1 (60.5%)
$\Delta E_{a_2}^c$				0.0 (0.0%)	0.0 (0.0%)	0.0 (0.0%)
$\Delta E_{b_1}^c$				–0.2 (0.3%)	–0.2 (0.2%)	–0.2 (0.3%)
$\Delta E_{b_2}^c$				–0.1 (0.1%)	–0.1 (0.1%)	–0.1 (0.2%)
$\Delta E_{e(\pi)}^c$				–40.2 (42.8%)	–36.1 (42.1%)	–31.0 (39.0%)
ΔE_{Prep}	5.8	4.3	4.0	5.4	4.6	4.0
$\Delta E (= -D_e)$	–45.1	–45.3	–47.1	–52.6	–51.6	–53.8

^a Energies in kcal/mol. ^b Values in parentheses give the percentage contribution to the total attractive interaction ($\Delta E_{\text{Elstat}} + \Delta E_{\text{Orb}}$). ^c Values in parentheses give the percentage contribution to the total orbital interaction (ΔE_{Orb}).

comes from the larger preparation energy, which is much higher (11.1 kcal/mol) than for the other compounds where the ΔE_{prep} values are between 4.3 and 4.5 kcal/mol. The instantaneous interaction energy ΔE_{int} in the fluorine compound is actually slightly stronger than in the other species.

We also compare the bonding situation of the bridging OC and **1RuC** ligands in Fe₂(CO)₉ and Fe₂(CO)₈(**1RuC**). Table 9 shows the EDA results for the (μ_2)OC–Fe₂(CO)₈ and (μ_2)**1RuC**–Fe₂(CO)₈ interactions. The bridging CO ligand has a higher BDE than the **1RuC** ligand, but the preparation energy

of (μ_2)**1RuC**–Fe₂(CO)₈ is also higher than that of Fe₂(CO)₉. The calculated interaction energies ΔE_{int} indicate that the strength of the bonding interactions of the two ligands is very similar. Both bridging ligands are slightly more electrostatically than covalently bonded. The (μ_2)OC–Fe₂(CO)₈ π -backdonation is larger than the (μ_2)**1RuC**–Fe₂(CO)₈ π -backdonation, which is similar to the EDA results for the terminally bonded ligands.

The IR spectra of carbonyls are an important tool to probe the electronic structure of TM carbonyl complexes. In Table

Table 8. Energy Decomposition Analysis of the **XRuC–W(CO)₅** (**X** = 1, 5, 6, 7) Bond in *C*_{2v} Symmetry at BP86/TZ2P//BP86/TZVPP^a

	5RuC–W(CO)₅		1RuC–W(CO)₅		6RuC–W(CO)₅		7RuC–W(CO)₅	
ΔE_{int}	–50.8		–49.7		–49.3		–48.9	
ΔE_{Pauli}	110.2		110.0		109.7		108.9	
$\Delta E_{\text{Elstat}}^b$	–90.1	(56.0%)	–85.8	(53.7%)	–84.7	(53.3%)	–82.9	(52.5%)
ΔE_{Orb}^b	–70.8	(44.0%)	–73.9	(46.3%)	–74.3	(46.7%)	–74.9	(47.5%)
$\Delta E_{a_1(\sigma)}^c$	–45.5	(64.2%)	–45.8	(62.0%)	–45.9	(61.8%)	–45.7	(61.1%)
$\Delta E_{a_2(\delta)}^c$	–0.3	(0.4%)	–0.3	(0.4%)	–0.3	(0.3%)	–0.3	(0.4%)
$\Delta E_{b_1(\pi)}^c$	–11.4	(16.1%)	–13.1	(17.7%)	–13.3	(17.9%)	–13.6	(18.1%)
$\Delta E_{b_2(\pi)}^c$	–13.7	(19.3%)	–14.7	(19.9%)	–14.9	(20.0%)	–15.3	(20.4%)
ΔE_{Prep}	11.1		4.3		4.4		4.5	
ΔE (=– <i>D_c</i>)	–39.7		–45.3		–44.8		–44.3	

^a Energies in kcal/mol. ^b Values in parentheses give the percentage contribution to the total attractive interaction ($\Delta E_{\text{Elstat}} + \Delta E_{\text{Orb}}$). ^c Values in parentheses give the percentage contribution to the total orbital interaction (ΔE_{Orb}).

Table 9. Energy Decomposition Analysis of the **1RuC–Fe₂(CO)₈** and the **OC–Fe₂(CO)₈** Bond in *C*_{2v} Symmetry at BP86/TZ2P//BP86/TZVPP^a

	1RuC–Fe₂(CO)₈		OC–Fe₂(CO)₈	
ΔE_{int}	–75.1		–78.4	
ΔE_{Pauli}	152.3		149.2	
$\Delta E_{\text{Elstat}}^b$	–109.1	(48.0%)	–104.0	(45.7%)
ΔE_{Orb}^b	–118.2	(52.0%)	–123.7	(54.3%)
$\Delta E_{a_1(\sigma)}^c$	–63.8	(53.9%)	–53.6	(43.3%)
$\Delta E_{a_2(\delta)}^c$	–1.2	(1.0%)	–0.8	(0.6%)
$\Delta E_{b_1(\pi)}^c$	–41.5	(35.1%)	–53.9	(43.5%)
$\Delta E_{b_2(\pi)}^c$	–11.7	(9.9%)	–15.5	(12.5%)
ΔE_{Prep}	52.4		49.1	
ΔE (=– <i>D_c</i>)	22.7		29.3	

^a Energies in kcal/mol. ^b Values in parentheses give the percentage contribution to the total attractive interaction ($\Delta E_{\text{Elstat}} + \Delta E_{\text{Orb}}$). ^c Values in parentheses give the percentage contribution to the total orbital interaction (ΔE_{Orb}).

S2, we list the calculated (BP86/TZVPP), unscaled frequencies for the C–O-stretching mode of the *trans*-CO ligand in L–W(CO)₅ (L = **1FeC**, **1RuC**, **1OsC**, **10FeC**, **10RuC**, **10Os**) in comparison to W(CO)₆. We observe for all LW(CO)₅ a shift of the frequency to smaller wavenumbers in the range of 14–27 cm^{–1} as compared to the parent W(CO)₆. We also performed EDAs of the LW(CO)₄–*trans*-CO bond to connect the shift in the C–O-stretching frequency with the σ -donor- and π -acceptor strength of the *trans*-CO ligand (see Table S3). It turned out that the ratio $\Delta E_{\text{orb}}(\sigma)/\Delta E_{\text{orb}}(\pi)$ correlates quite well with the observed stretching frequencies for a given group of complexes (**1MCW(CO)₅** and **10MC(WCO)₅**). This is shown in Figure S2 in the Supporting Information. Overall, these observations corroborate the finding that the carbon complexes have a higher σ -donor/ π -acceptor ratio than does CO.

Summary and Outlook

The results of this study clearly predict that the transition metal carbon complexes [(X₂(R)₂M(C))] of the group-6 elements M = Cr, Mo, W with X = halogen and R = PR₃ or NHC should

exhibit a ligand behavior that is akin to isolobal carbon monoxide. The bond strength and the donor–acceptor properties of metal carbon complexes closely resemble those of CO, and thus carbon complexes may be considered as electronically tuneable analogues of carbon monoxide. Similar properties are also calculated for the porphyrin carbon complexes **10MC**, which bind more strongly and are slightly stronger π acceptors than the [(X₂(R)₂M(C))] species. The carbon complexes [(X₂(R)₂M(C))] are slightly weaker π acceptors than CO, and thus they tend to have a bit weaker bonds than CO in group-6 donor–acceptor complexes. The calculations suggest that bond energies of carbon complexes as ligands with d¹⁰ transition metals are larger than those of CO. The theoretical results let it seem possible that adducts with more than one carbon complex as ligands may become synthesized and that even homoleptical complexes may be prepared.

Acknowledgment. This work was financially supported by the Deutsche Forschungsgemeinschaft.

Supporting Information Available: Table S1 gives the Cartesian coordinates (in Å) and total energies of all compounds discussed in the text. Table S2 gives the unscaled C–O stretching frequencies of the *trans*-CO ligand in L–W(CO)₅ (L = **1FeC**, **1RuC**, **1OsC**, **10FeC**, **10RuC**, **10Os**) and W(CO)₆. Table S3 gives the results of EDA calculations of the LW(CO)₄–*trans*-CO bond in L–W(CO)₅ (L = **1FeC**, **1RuC**, **1OsC**, **10FeC**, **10RuC**, **10Os**). Figure S1 shows the structures that are not given in Figures 1 and 4–6. Figure S2 shows the correlation of the C–O stretching frequency of the *trans*-CO group in LW(CO)₅ (L = CO, **1FeC**, **1RuC**, **1OsC**, **10FeC**, **10RuC**, **10OsC**) with the ratio of $\Delta E_{\text{orb}}(\sigma)/\Delta E_{\text{orb}}(\pi)$ for the *trans*-CO–W(CO)₄L bond. This material is available free of charge via the Internet at <http://pubs.acs.org>.

JA8047915